Final report

Food Standards Agency project M03063: Surface FIDA

Introduction

The pathological isoform of the host encoded prion protein (PrP^{Sc}) is strictly correlated with transmissible spongiform encephalopathies (TSE) like Scrapie in sheep or BSE in cattle. According to the prion model PrP^{Sc} is by itself the agent of the disease. In any case PrP^{Sc} is the earliest known biomarker of the disease and for this reason *a priori* will suit for diagnosis. PrP^{Sc} embodies a proteinase K (PK) resistant and PK-sensitive portion, and in contrast to the presently existing tests the sum of both portions would be the most sensitive parameter for testing. Both portions form insoluble aggregates, which cannot be detected in healthy animals; therefore aggregates of PrP^{Sc} are used as unequivocal markers for TSE. If it is possible to count single particle of aggregated PrP^{Sc}, either in tissue or in body fluids, one can approach the theoretical limit of TSE-diagnosis. With the method of surface-FIDA (fluorescence intensity distribution analysis on a surface, see fig. 1, which was developed in our group, we can come close to the theoretical limit of sensitivity.
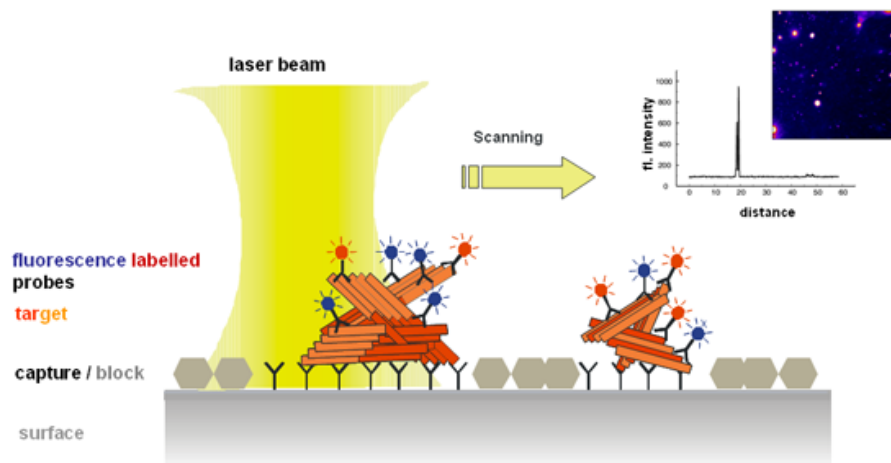
Fig. 1 surface-FIDA
Model of surface-FIDA

We developed this new method which is depicted in Fig.1. PrP^{Sc}-particles, the PK-sensitive as well as the PK-resistant portion, are bound to a surface via capture antibodies. The antibodies have not to be specific for PrP^{Sc} they have only to bind PrP^{Sc} with high affinity. The PrP^{Sc}-particles are labelled with two different antibodies carrying different fluorescent labels. The chip carrying the double-labelled PrP^{Sc}-particles is evaluated in a commercially available fluorescence correlation spectrometer (FCS) with dual colour mode (Evotec Technologies, Hamburg). A laser beam is scanning in a double-meander way the surface and produces a flash

whenever it hits a PrP^{Sc}-particle. The computer-aided evaluation system guarantees that only those flashes are counted as PrP^{Sc}-particle when both colours of the two different antibodies are detected simultaneously (crosscorrelation mode).

The method is based on four consecutive steps which are specific for PrP^{Sc}-particles.
- PTA-precipitation
- binding to capture antibody
- labelling by antibody 1
- labelling by antibody 2

In an earlier study (Birkmann et al. 2006) we have searched with the same instrument for double-labelled PrP^{Sc}-particles, but floating freely in solution. The chance of a PrP^{Sc}-particle to get detected in the focus of the laser beam was much lower and the results showed much more scattering. Applying, however surface-FIDA, the sensitivity to identify Scrapie-infected animals in samples from brain and body fluids could be increased dramatically as compared to FIDA in solution. Thus a highly sensitive and specific detection method is presently available.

Due to lack of sample material, we could examine only very few CSF samples of BSE-infected cattle in comparison to non-infected controls up to now. We could detect clearly PrP^{Sc}-particles in the CSF of BSE-afflicted cattle; but since only a few samples were analysed, we can presently not claim, that surface-FIDA is generally applicable for detecting BSE in CSF. Only the first essential steps towards a test on living animals were taken at that time.

The structure of PrP^{Sc} is not uniform. A portion of it is sensitive against digestion with Proteinase K (PK) like the cellular Isoform PrP^{C}, whereas the remaining portion of full-length PrP^{Sc} is N-terminally truncated by PK and the remaining C-terminal part containing amino acids 90-231 (sequence numbering according to hamster PrP), also called PrP27-30, is highly resistant against further PK-digestion while keeping full infectivity. Indeed, PK-resistance of PrP 27-30 is the basis of most commercially available tests, and the readout systems are ELISA or Western blots. We do not need to discuss the theoretical limitations of those tests because all empirical data show that on the one side they are routinely applicable but on the other side they are restricted to *post mortem* tests and to samples from brain tissue.

In order to raise the sensitivity of tests and maintain the specificity we studied other features of PrP^{Sc}. In the literature conformation dependent immunoassay (Safar et al. 1998; Safar et al. 2002) or conformation dependent antibodies (Paramithiotis et al. 2003), and other conformation specific ligands (Grosset et al. 2005) have been described. According to our studies the most sensitive feature of PrP^{Sc} *versus* PrP^{C} is the state of aggregation. That is for several reasons:

i)   Aggregates of PrP^{Sc} embody not only PK-resistant PrP27-30 but also PK-sensitive PrP^{Sc}. The ratio of both varies between tissues, states of disease and even individuals, and our preliminary studies showed examples of BSE-afflicted cattle with nearly no detectable PrP27-30 but with considerable amounts of aggregated PrP^{Sc}.

ii)   Aggregated PrP^{Sc} can be separated from PrP^{C} by PTA-precipitation. This is a well suited preparation step and works in lowest concentrations of PrP^{Sc}, since precipitation does not rely on PrP^{Sc}-PrP^{Sc} complexes which would depend on PrP^{Sc}-concentration but on PrP^{Sc}-PTA complexes.

iii)   PrP^{Sc}-aggregates can be detected by single particle counting. We have developed the method of single-particle-counting by fluorescence-correlation spectroscopy in solution (FIDA) (Birkmann et al. 2006) and lately improved the principle to single particle counting on a surface, so-called surface-FIDA (Birkmann et al. 2007).

iv)   The method of surface-FIDA involves several highly sensitive and specific steps.

         a. Capture of PrP^{Sc}-particles from solution to antibodies attached to the surface of a detection chip

         b. Labelling of the captured PrP^{Sc}-particles by two different antibodies, *i.e.* with different epitopes and different fluorescent labels

         c. Detection of crosscorrelating fluorescence signals by fluorescence spectroscopy (2D-FCS)

v)   The only principal prerequisite and theoretical limit of the method is the presence of a single PrP^{Sc}-particle in the sample volume (25µl) which is applied to the surface-chip.

Our group has developed the method to a level that in cerebrospinal fluid of BSE-afflicted cattle PrP^{Sc}-particles could be detected, whereas only negative reports were described in the literature (Buschmann and Groschup 2005). Consequently the principle of a test on living animals although not suitable for routine testing, could be shown already, but systematic optimisation and serial tests, also of blinded samples are needed to demonstrate the reliability of the test system and its applicability to other body fluids, most important blood, possibly but less probable urine.

We have also developed an amplification procedure prion protein amplification (PPA) similar to that described by the Soto group (Soto et al. 2002), but clearly different in the sense that no cell extracts but only purified components like recombinant PrP (recPrP) and buffer are applied. The amplification procedure has to be evaluated very critically as a test system, because the amplification is entirely dependent upon the presence of PrP^{Sc} as seed, and false positives as a consequence of spontaneous

aggregation and amplification which is possible and has been shown experimentally, have to be avoided strictly. The PPA-method is based on the seeded amyloid fibril formation of PrP; it was established in our group for *in vitro* amplification of PrP-particles. PrP-particles were purified from Scrapie-infected hamster brain with PTA precipitation and recPrP monomers were added under well selected conditions. These conditions guarantee that the monomers were in a transition state as determined by us in an earlier work (Leffers et al. 2005), patent # 02 722 213.2-2403 and DE 102005031429.5). It should be emphasized that our amplification system is clearly different from that of the Soto group (Saborio et al. 2001) as only purified components are applied, *i.e.* no cellular extract. Only in the presence of PrP^{Sc}-particles specific fibril formation can be observed as analysed by Thioflavin T (ThT) fluorescence and electron microscopy. PrP-particles could be detected in amounts down to 2.5×10^{-5} brain equivalents. It should be noted, that such an amplification system was developed first in our group to detect Alzheimer disease specific seeds for Abeta-fibrilliogenesis (Pitschke et al. 1998).

Combination of such an amplification procedure with surface-FIDA as detection system should result in an ultrasensitive detection method for TSE-associated particles. The amplification or even growing steps could be important, if the number of particles is very low and/or the particles are small. Both could be the case in the early state of disease and in non-CNS-tissues or body fluids. In that case the PPA leads to a growing of the particles in the first step (seeded aggregation) and to an enhancement of the number of particles by cyclic amplification, but cyclic amplification is not a prerequisite.

During the time course of this project also other groups made major advances in the diagnostic field of prion diseases using body fluids. Due to applying protein misfolding cyclic amplification (PMCA) it was possible to detect PrP^{Sc} in blood from prion-infected hamsters, sheep and deer (Saborio et al. 2001, (Murayama et al. 2007; Thorne and Terry 2008; Rubenstein et al. 2010). However, since PrP^{C} in the brain homogenate substrate can also aggregate spontaneously, PMCA bears the risk of false-positive results and might therefore not be optimal for diagnostic purposes.

Without the use of *in vitro* amplification and protease digestion, PrP^{Sc} could be detected in the peripheral mononuclear blood cells of scrapie-afflicted sheep, even in pre-clinical animals (Terry et al. 2009). Recently, remarkable progress has been made in the field of CJD diagnostics. In a blinded study, 71% of variant CJD positive blood samples could be identified by sensitive immune detection of surface captured prions (Edgeworth et al. 2011). Similar sensitivity was achieved by subjecting CSF samples of patients with sporadic CJD to an *in vitro* amplification technique, termed real-time quaking-induced conversion (Atarashi et al. 2011).

Material and Methods

We only document the standard methods in this chapter, because the detailed protocols of sample preparation and surface-FIDA measurements were part of the method development and are documented in the result chapter.

Standard Buffers

Phosphate buffered saline (PBS)
137   mM   NaCl
2.7   mM   KCl
8.1   mM $Na_2HPO_4 \cdot 2\,H_2O$
1.76   mM KH_2PO_4
pH 7.4

PBSTT
PBS supplemented with 0.1% Triton X-100 and 0.1% Tween-20

Protein gel electrophoresis (SDS-PAGE)

Protein gel electrophoresis was carried out in a Hoefer SE 600 chamber by Amersham Pharmacia Biotech (San Francisco, USA) according to the protocol of Laemmli (Laemmli et al. 1970). Gel electrophoresis was carried out in 1x Laemmli buffer in the presence of 0.1% SDS for 30 minutes at 180 V followed by approximately 90 minutes at 220 V or until the bands had reached the desired position in running the gel. As marker the "Benchmark Prestained Protein Ladder" (Gibco BRL, USA) was used.

10 x gel electrophoresis buffer (10 x Laemmli buffer)
1.9 M Glycine (288 g)
0.25 M Tris (60 g)
ad 2 l distilled water
pH will adjust to 8.3

Stacking gel
124 mM Tris/HCl pH 6.8
3% Acrylamide/Bisacrylamide (30:0.8)
0.1% SDS
0.1% TEMED
0.1% APS

Running gel (12%)
380 mM Tris/HCl pH 8.8
12% Acrylamide/Bisacrylamide (30:0.8)
0.1% SDS
0.1% TEMED
0.1% APS

Sample buffer (2x)
62.5 mM Tris/HCl pH 6.8
5% SDS
10% Glycerol
0.016% Bromphenolblue

Western Blot blot

Western blotting was performed as described in Panza et al. 2010. Detection of the prion protein was carried out using antiPrP antibody SAF 32 diluted 1:5,000 in TBST (10 mM Tris–HCl [pH 8.0], 150 mM NaCl, 0.1% Tween20). Detection was performed with peroxidase-conjugated goat-anti-mouse secondary antibody (Jackson ImmunoResearch, Newmarket, Suffolk, UK) and the immunoreactive bands were visualized with SuperSignal West Pico chemiluminescent substrate (Thermo Scientific, Rockford, IL, USA).

Recombinant Prion Proteins

The recombinant prion protein (recPrP) was prepared and purified as described by Leffers et al. (2005). The recPrP with the amino acid sequence of cattle (25-241) (BovPrP) PrP was used in our studies before. We adapted the purification protocols to full length recombinant ovine PrP (25-233) (OvPrP).

PTA precipitation of PrP^{Sc}

PTA precipitation was carried out to precipitate PrPSc and leave PrP^{C} in the supernatant. Up to 2 g of brain tissue was diluted to 30% (w/v) in PBS pH 7.4 containing a protease inhibitor mix (complete mini, EDTA-free, Roche, Mannheim, Germany) by homogenising with a PowerGen homogeniser (Fisher Scientific, Schwerte, Germany) for 30 s on minimum power level. One volume of PBS pH 7.4 with 4% (w/v) for Scrapie samples and 8% for BSE samples sarkosyl was added and mixed for another 30 s at maximum power level. The resulting homogenates were diluted with PBS containing 2% for Scrapie samples and 4% sarkosyl for BSE samples (w/v) sarkosyl to a final concentration of 5% (w/v) and mixed for 10 s. The brain homogenates were frozen immediately after preparation and stored at -70 °C. After thawing of brain homogenates, gross cell debris was removed by centrifugation for 5 min at 5,000 x g. The prepurification of PrP^{Sc} from brain homogenate is based on the PTA precipitation protocol of Safar and colleagues (Safar et al. 1998). The applied protocol was modified and consists of two successive PTA precipitations

without MgCl$_2$. The resulting PTA precipitate was washed with 200 µl of PBS containing 0.2% sarkosyl (w/v). After incubating for 30 min on a rocking platform at 37 °C the samples were centrifuged at 14,000 x g (Centrifuge 5415 R, Eppendorf, Hamburg, Germany) for 30 min. The resulting PTA-pellet was re-suspended in PBS by sonication for 40 s at level 7 in a sonicator bath (Sonicator 3000, Misonix, Farmingdale, NY, USA) and 2 s with a sonication lobe at 25 W (Bandelin sonopuls, Bandelin electronic, Berlin, Germany). Different treatments of brain tissues and body fluids are indicated in the chapter results

Fluorescence labelling of antibodies
Antibodies were labelled with Alexa Fluor-633 or -488 dye using the Protein Labelling Kit (Invitrogen, Carlsbad, Californien, USA). Labelled antibodies were stored in PBS containing 25% glycerine and 1.5% BSA (w/v) in the dark at 4 °C.

Circular dichroism spectroscopy
Circular dichroism (CD) spectra were recorded with a J-715 spectropolarimeter (Jasco, Easton, MD, USA) in a 0.1 cm quartz cuvette at room temperature. The scanning speed was 50 nm/min with resolution of 1 nm. For each sample 10 spectra were accumulated between 195 and 260 nm. The protein concentration was 150 ng/µl. Background spectra of buffer samples were subtracted from the respective protein spectra.

Electron microscopy, negative stain
A droplet of 5-10 µl containing the recPrP was placed on glow discharged grid and left to adsorb for 2 minutes. After adsorption to the grid surface the sample was washed briefly (50 µl of: 0.1 and 0.01 M NH$_4$ acetate) and stained with 2% ammoniummolybdate (50 µl). The samples were analysed with a Zeiss EM910 microscope at 80 kV.

Congo red staining
A 10 µl aliquot of the fibril samples containing preformed fibrils was applied to gelatin coated glass slides and stained with Congo red according the protocol described by Müller et al. (2007). Picture of the samples were taken with the "Polarisationsphotomikroskop III" (Carl Zeiss, Oberkochen, D)

Thioflavin T-Assay
Fluorescence emission spectra of Thioflavin T were measured at a concentration of 5 µM ThT and 10 ng/µl recPrP in 150 µl 10 mM NaPi pH 7.4. The emission spectra were recorded from 460 nm to 630 nm with a fixed excitation wavelength of 455 nm, average of emission intensity between λ_{em} 495 to 505 is shown for a time point. Fibrillogenesis kinetics were followed in 96 well plates according to Stöhr et al. (2008). All measurements were performed in a Tecan saphire plate reader (Tecan

Group, Maennedorf, Switzerland). The chosen regression line is polynomial fitted to original data points.

Spontaneous and seeded amyloid formation of recPrP

Spontaneous and seeded amyloid fibril formation of recPrP of the different species was monitored by ThT-assay as described above. The buffer conditions, especially the SDS-concentrations, were adjusted according to the amyloid forming conditions of the spontaneous case for each species. The results are displayed as sum of the average fluorescence intensity of 495 to 505 nm in the saturation phase (24h to 48h in 30 min interval) of the curve. To determine the specificity of the seeding effect PTA-precipitated PrP^{Sc} from brain tissue of infected and non-infected animals was compared.

Brain tissue and body fluids

Brain and blood material was generously provided by the followings institutes:
   i)   Pathogenesis study BSE brain and blood fractions as well as CSF – Martin Groschup, FLI, Insel Riems
   ii) Brain and blood from sheep naturally infected with scrapie – Jan Langeveld, CVI, Lelystad
   iii) Plasma from clinical sheep – Linda Terry and Sally Everest, VLA, Weybridge
   iv) Coded panel of plasma samples – Maurice Bardsley, TSE archives, VLA, Weybridge
   v)   Brain and blood samples from scrapie sheep – Emanuel Comoy, CEA, Fontenay-aux-Roses
   vi) Brain from scrapie confirmed sheep – Olivier Andreoletti, INRA-ENVT, Chemin des Capelles

Antibodies

Antibodies were provided by:
   i)   L42 – Jan Langeveld, CVI, Lelystad
   ii) W261 – Lothar Stitz, FLI, Insel Riems
   iii) FH11 – C.R. Birkett, IAH, Compton
   iv) Saf32 – purchased from SPI-Bio

Results

We optimised every step of the surface-FIDA assay.

Optimisation of the surface coating

First we optimised the surface coating from the former protocol of adhesive attachment of the capture antibody to the glass surface covered with Poly-D-lysine to a covalently linkage of the antibody to the surface by spacers. Therefore we tested for different covalent coating procedures:

1. *Glutaraldehyde*

The first spacer we tested was the homobifunctional glutaraldhyde with is able to bind aminogroups on both sites. We established a covalent binding protocol, but the resulting surface confronted us with a new problem. The surface modification with gnalysedlutaraldehyde leads to a dramatic increase of autofluorescence.

2. *Sulfosuccinimidyl 4-(N-maleimidomethyl)cyclohexane-1-carboxylate (Sulfo-SMCC)*

Sulfo-SMCC is heterobifunctional and allows covalent conjugation of amine- and sulfhydryl-containing molecules. Therefore the capture antibody had to be cleaved for presenting a sulfhydryl group. The advantage would be a site-specific attachment of the capture. But a disadvantage was the time consuming procedure of the attachment and the leakage of the capture after cleaving.

3. *Cyanogenbromid*

A short immobilization protocol was envisaged with this very short heterofunctional spacer. But it could not be realized because the assay chips were not composed of polypropylene but of polystyrol which is less resistant to solutions required for the immobilization reaction.

4. *PEG*

Finally we tested a poly-ethylene-glycol [PEG] derivate N-hydroxysuccinimid – PEG – Carboxyl [NHS-PEG-COOH]:

$$\text{N}-\text{O}-\overset{\overset{\text{O}}{\|}}{\text{C}}\text{O}(\text{CH}_2\text{CH}_2\text{O})\text{n}\text{CH}_2\overset{\overset{\text{O}}{\|}}{\text{C}}\text{OH}$$
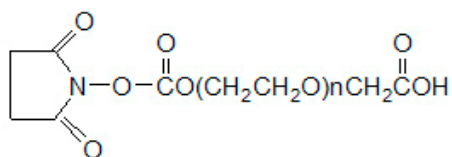
This homobifunctional spacer is very flexible (molecular weight: 3,400 Da), and its hydrophilic properties avoid unspecific attachment of biological tissue to the glass-surface. The glass surface was activated with ethanolamine and the resulting amino

group is bound by the NHS-group of the PEG. Then the carboxy group on the other end of the molecule is activated with a mixture of N-hydroxysuccinimide [NHS] and 1-Ethyl-3-(3-dimethylaminopropyl) carbodiimide [EDC] allowing the covalent binding of an amino group of the capture antibody (fig. 2).
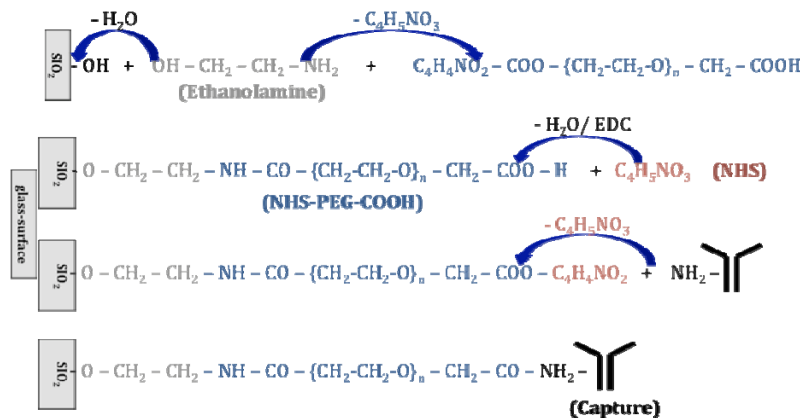
Fig. 2 chemical reaction crosslink the capture antibody to the glass surface by PEG

We controlled the binding of the capture with a fluorescence labelled secondary antibody, which recognizes the capture antibody. After the modification of the glass-surface of the assay chips the capture was added and a chip without capture antibody served as control (fig. 3). We could successfully establish a covalent binding of the capture antibody to the glass surface. A model for the resulting antibody coated surface is shown in figure 4. A detailed experimental protocol is listed below.
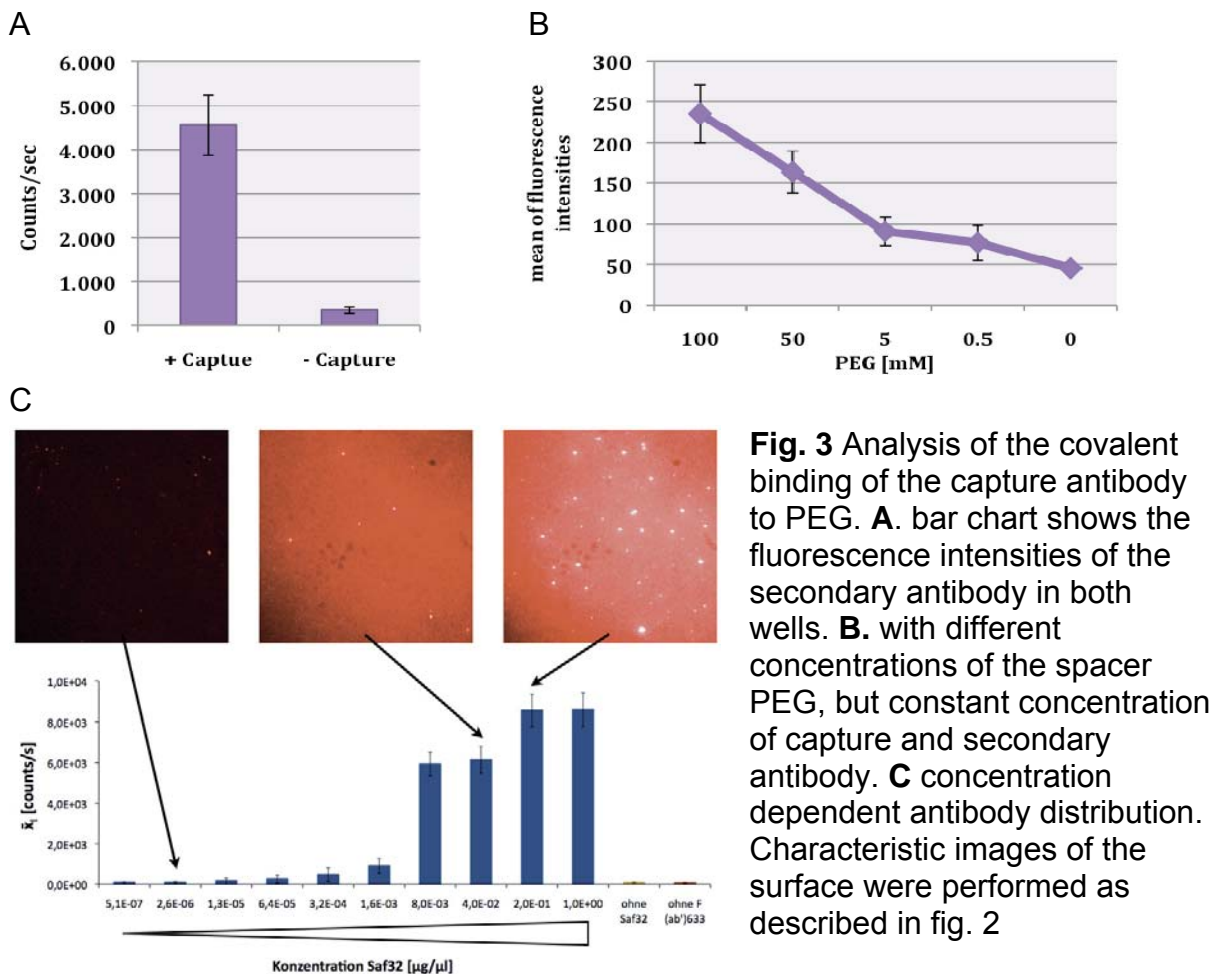
Fig. 3 Analysis of the covalent binding of the capture antibody to PEG. **A**. bar chart shows the fluorescence intensities of the secondary antibody in both wells. **B.** with different concentrations of the spacer PEG, but constant concentration of capture and secondary antibody. **C** concentration dependent antibody distribution. Characteristic images of the surface were performed as described in fig. 2

10

Protocol to bind the capture antibody covalently to a glass surface

Standard fill of wells: 100 µl

1. Pre-treatment of the glass-surface
- 15 min NaOH (5M)
- wash: 3 x H_2O
- 15 min HCl (1M)
- wash: 3 x H_2O and 2 x ethanol
- dry with nitrogen

2. Activation of glass (amino groups)
- 30µl ethanolamine (5,6M) incubation overnight
- 4 x DMSO and 2 x ethanol
- dry with nitrogen

3. Addition of the Spacer PEG
- 10µl PEG (solubilize 17mg PEG in 100µl of DMSO + 2µl of triethylamine) incubation: 1h or overnight
- wash: 5 x H_2O

4. PEG-Activation
- 30µl NHS/EDC (50mM) incubation: 30 min – max. 1 h
- wash: 3 x MES

5. Covalent binding of capture antibody
- 10µl Capture (50 - 100 ng/µl) in PBS incubation: 1 - 2 h
- wash: 4 x PBS

6. Blocking I
- 50 – 100 µl 3% BSA 30 mM triethylamine in PBS incubation: 1 h or overnight
- wash: 3 x PBSTT and 3 x PBS

7. Target
- 20µl target incubation 2 h or overnight at 4°C
- wash: 4 x PBS 0.2% SDS and 4 x PBSTT and 4 x PBS

8. Blocking II
- 50 – 100 µl 1.5% BSA in PBS incubation: 1 h
- wash: 4 x PBS 0.2% SDS and 4 x PBSTT and 4 x PBS

9. Fluorescence labelled antibodies
- 15µl of supernatant after 1h 100.000 x g of antibody mixture (1ng/µl, 1.5% BSA; PBS) incubation ca. 1 - 2 h
- wash: 4 x PBSTT and 4 x PBS
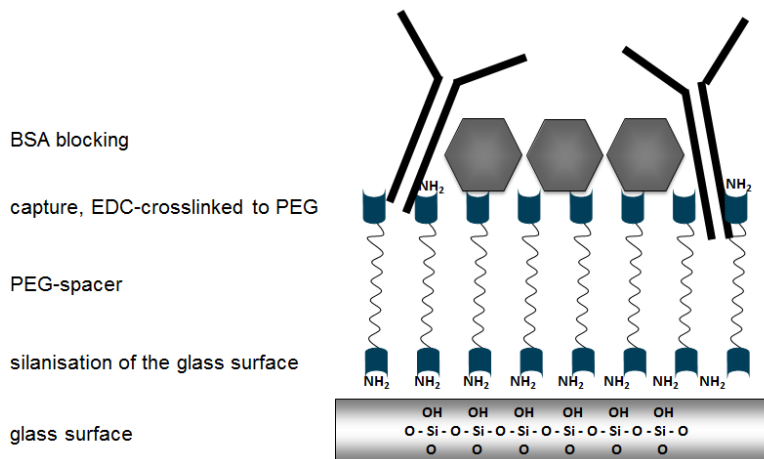
Fig. 4 Model of antibody coated glass surface

Optimization of washing and blocking steps after binding PrP^{Sc}-aggregates to the chip surface

The covalent linking of the capture antibody to the glass surface allows us to apply harsh washing conditions without removing the capture antibody. After loading the prion sample and consecutively the detection antibodies, we routinely washed the wells with an excessive volume of PBS containing 0.1% Triton-X 100 and 0.1% Tween20. In the case of PTA precipitated brain homogenate these washing conditions turned out to be insufficient, as non-specific aggregates in the negative samples could not be removed efficiently (figure 5). In fig. 5 brain preparations from non-infected animals were used and the background was high, with a signal even higher than in case of samples form Scrapie-infected animals. Thus, we washed more stringently with PBS containing the ionic detergent SDS. Employing 0.2% SDS during incubation of PrP^{Sc} purified from brain homogenate (0.2% SDS target) or after application of detection antibodies (0.2% SDS 2. wash) led to a dramatic loss of signal. However, washing with 0.2% SDS immediately after target incubation enabled a good differentiation of the positive from the negative samples. The increase of the signals in the Scrapie sample compared to that without washing steps could be explained by masking effect of the impurities on PrP^{Sc} epitopes.

1,20E+07

1,00E+07

8,00E+06

6,00E+06

4,00E+06

2,00E+06

0,00E+00

fluorescences intensity > cutoff

1) 2) 3) 4)

| pos | neg | pos | neg | pos | neg | pos | neg |
| PTA bh | | 0.2 % SDS target | | 0.2 % SDS 1. wash | | 0.2 SDS 2. wash | |

	1)	2)	3)	4)
	PBS	**0.2% SDS**	PBS	PBS
	0.1% Tween20 &TritonX	0.1% Tween20 &TritonX	**0.2% SDS**	0.1% Tween20 &TritonX
	PBS 1.5% BSA	PBS 1.5% BSA	PBS 1.5% BSA	PBS 1.5% BSA
	0.1% Tween20 &TritonX	0.1% Tween20 &TritonX	0.1% Tween20 &TritonX	**0.2% SDS**

surface with covalently linked capture
(blocked with BSA)

↓

loading PTA precipitated brain homogenate

↓

1st wash

↓

incubation of detection antibodies

↓

2nd wash

Fig. 5: Analysis of different washing steps in the surface-FIDA assay, PrP^{Sc} purified from brain homogenate (pos) and identically treated negative controls (neg) were compared. The fluorescence above a cut off of 500 was integrated.

Coating of the glass chip with PEG results in a hydrophilic surface, which suppresses hydrophobic interactions with impurities. After linking of the capture, a treatment with 3% BSA in PBS was useful to block remaining non-specific binding sites of the glass surface. After sample loading a second blocking step with 1.5% BSA was introduced, to prevent non-specific interactions with the detection antibodies. Alternatively, BSA could be applied directly in the detection antibody incubation.

Optimization of the capture/probe combination for PrP^{Sc}-particles

As depicted in Figure 7, mouse antibodies FH11 (Foster et al. 1996) and Saf32 (purchased from SpiBio) yielded best results with respect to sensitivity and specificity. It should be noted that both antibodies bind to the N-terminal portion of the prion protein, which is believed to be exposed in the aggregated state of PrP. Therefore we chose this pair of detection antibodies for our dual color measurements.

Saf32 was also used as the covalently bound capture, which further increased specificity of the assay, because Saf32-captured monomeric PrP cannot be detected by the same antibody.
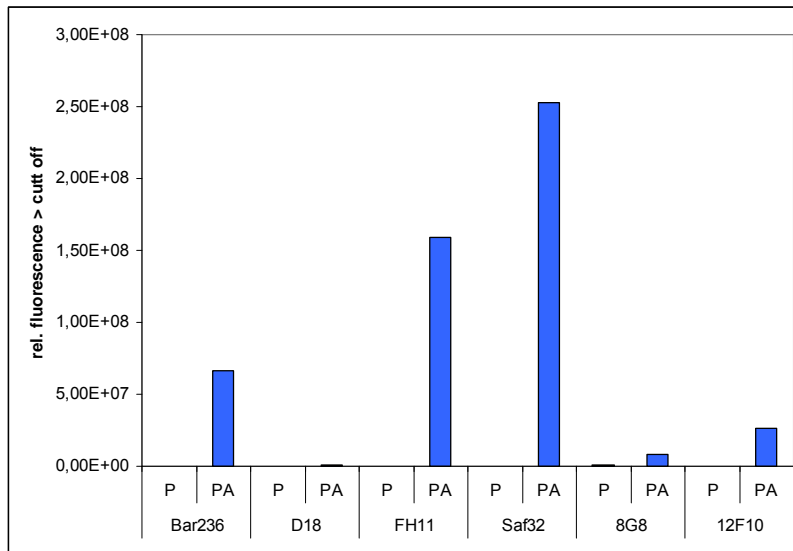
Fig. 6:
analysis of different antibodies in the surface-FIDA assay
The fluorescence above a cut off of 500 was integrated.
P: plasma; PA: Plasma spiked with sheep recPrP aggregates.

Optimization of the preparation of brain tissue and body fluids depending on the different species:

a) **Brain tissue from sheep with clinical scrapie**

Precipitation with phosphotungstic acid (PTA) is commonly used for both concentrating and purification of prions from brain homogenate (Safar et al. 1998). The amount of precipitated PrP^{Sc} depends on the PTA concentration. In preliminary experiments we determined the optimal PTA concentration with respect to maximum yield of PrP^{Sc} and minimum background from PrP^{c}. We found that at 0.25% PTA high amounts of PrP^{Sc} could be recovered, while no detectable level of PrP^{c} is seen by western blot analysis (fig. 7). In contrast, in 0.4% PTA also weak signals of PrP^{C} are detectable.
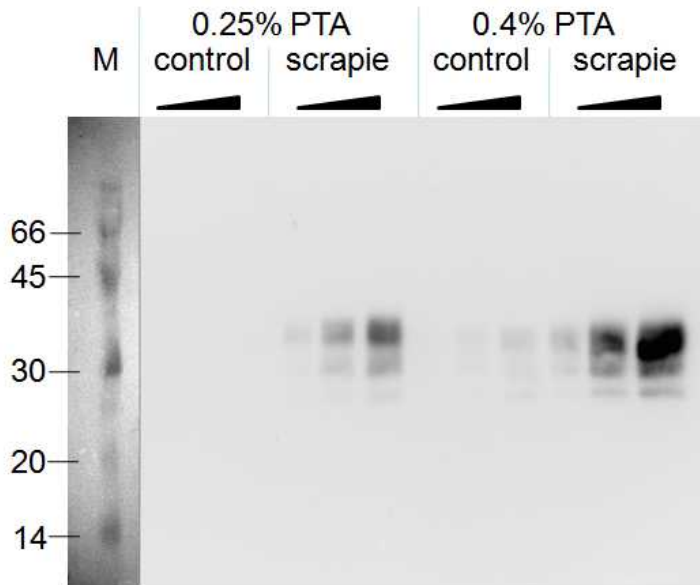
Fig. 7:
Purification of PrP^{Sc} from sheep brain homogenate. Increasing amounts of brain homogenate are shown by the triangle. Differences between the two controls are more evident on original exposures.

We initially considered a mild digestion with proteinase K in order to reduce background signals. Surprisingly, almost all of the PrP^{Sc} was sensitive to proteinase K concentrations even as low as 0.5 µg/ml (fig. 8).
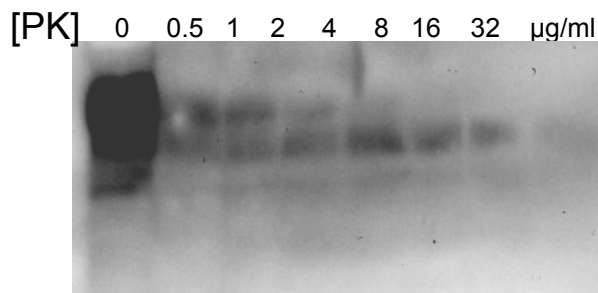
Fig. 8
Digestion of PrP by proteinase K in ovine Scrapie brain homogenate

b) Blood plasma from sheep with clinical scrapie - establishing purification by spiking with rec PrP aggregates

When measuring recPrP spiked in ovine plasma it became obvious, that signal intensities drastically decreased (Figure 9, 2nd panel). This is probably due to the high content of low density lipoprotein (LDL) in the plasma fraction. It was previously described that LDL is associated with human prions (Safar et al. 2006), suggesting that also recPrP is masked by LDL particles in ovine plasma, and thus the epitopes are masked against detection antibodies. To address this issue we optimised our preparation protocol by treating samples with sarkosyl followed by a lipase digestion in order to dissociate the PrP/LDL complexes. Addition of sarkosyl results in a moderate increase of fluorescence intensities (barely visible in fig. 9, 3rd panel). The optimal mixture of lipases was suggested by Prof. Jäger (Heinrich-Heine-Universität Düsseldorf)Signals are significantly boosted when samples were additionally treated

with a mixture of Phospholipase A, Phospholipase C, and CalB-Lipase (fig. 9. 4th panel). Finally, PrP aggregates could be fully recovered and concentrated by precipitation with PTA (fig. 9, 5th panel). A detailed protocol of the plasma preparation is described below.
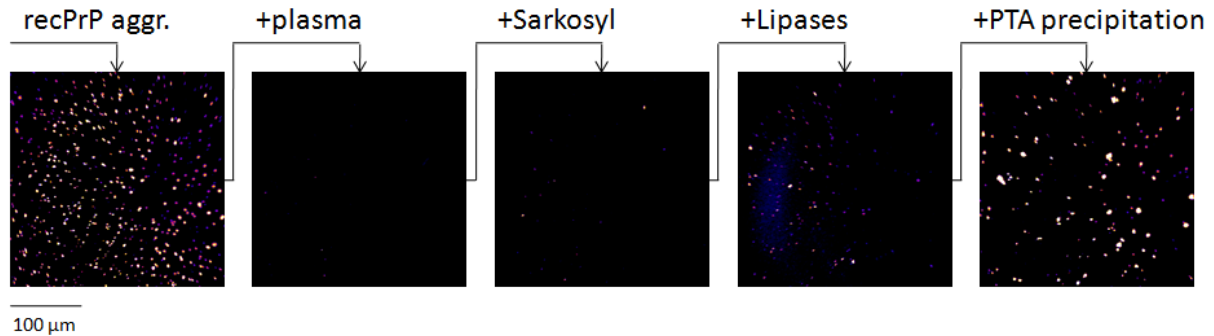
Fig. 9 Purification and enrichment of aggregates of recPrP from blood plasma

Protocol for the preparation of sheep blood plasma
- 200 µl ovine plasma
- adjust to 2% sarkosyl
- 37°C, 15 min
- add 1U of each Phosholipase A, C and CalB Lipase
- 37°C, 45 min
- adjust to 0.25 - 0.36% PTA
- centrifuge 16,000 g, 20 min, 25°C
- wash pellets with 200 µl PBS
- recentrifuge
- resuspension of the pellets in 40 µl PBS by ultrasonication
- Incubation overnight on capture surface, 4°C

c)   **Peripheral mononuclear blood cells from sheep with clinical scrapie**

On the basis of the comparison from the literature of samples from plasma and from peripheral mononuclear blood cell (PBMC) it appears more promising to carry out serial measurements with PBMC samples.

We regarded analysis of this fraction as most promising to bring forward our test. Furthermore, PrP^C content in the PBMCs is sufficiently high to track disposition of PrP^C in the sample pre-purification by western blot analysis (Thackray et al. 2006).

In initial experiments we observed that after thawing, PBMC samples became extremely viscous due to release of genomic DNA. To counteract this we employed treatment with benzonase which hydrolyses all nucleic acids, and thus reduces medium viscosity. Cell lysis was supported by adjusting samples to 2% sarkosyl.

With these preparation step PTA precipitation could be applied. It was checked by western blot analysis that PrP^C remains in the supernatant and no PrP^C is found in the pellet neither in Scrapie-negative nor in positive PBMC sample (figure 10). However, from these analyses it is also evident that PrP^C content in the PBMC fraction can differ significantly between individuals (compare S3 *vs* S4). It should be noted that PrP^{Sc} in the pellet cannot be detected in the western blot (fig. 10) due to the limited sensitivity of the western blot method.
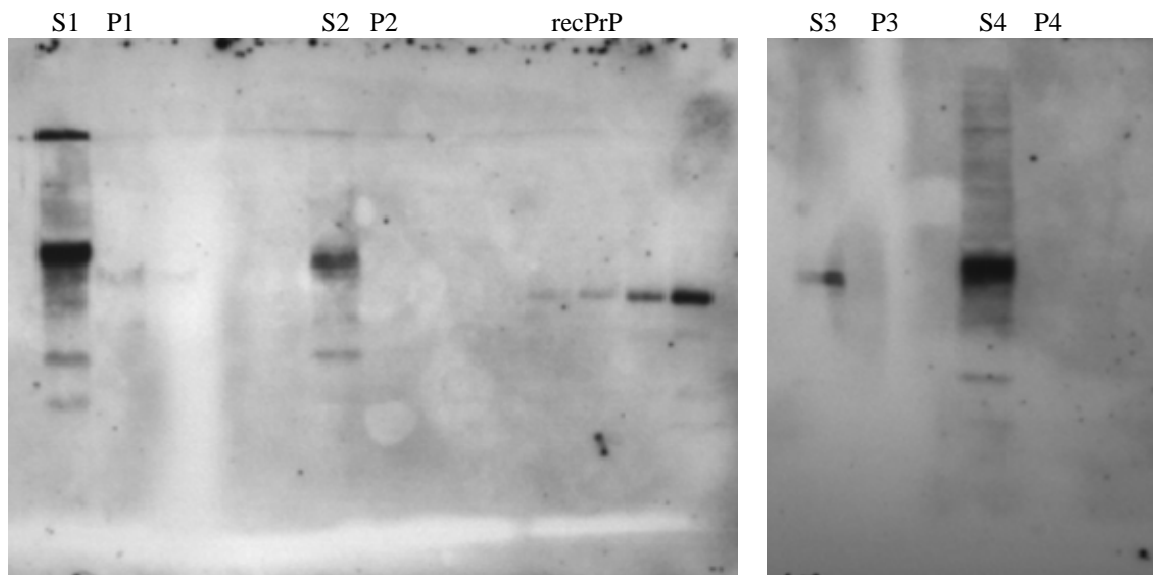
Figure 10: Western blot analysis of PTA precipitated PBMC fractions. Two scrapie-positive (1,2) and two negative (3,4) PBMC samples were precipitated with PTA. Supernatants (S) and pellets (P) were analysed for PrP^C by western blot analysis. Amounts of rec PrP: 0.13, 0.25, 0.5, 2.5 ng

To determine whether PrP^{Sc} aggregates can be enriched in PBMC environment by PTA precipitation, we conducted spiking experiments using brain homogenate from Scrapie-infected and control sheep. Results are shown in figure 11. As expected, PBMC spiked with negative brain homogenate only yields a signal in the supernatant (lane 2), whereas PrP^{Sc} from Scrapie brain homogenate is efficiently precipitated (lane 4). These results demonstrate that PTA-precipitation can also be applied to PBMC samples.
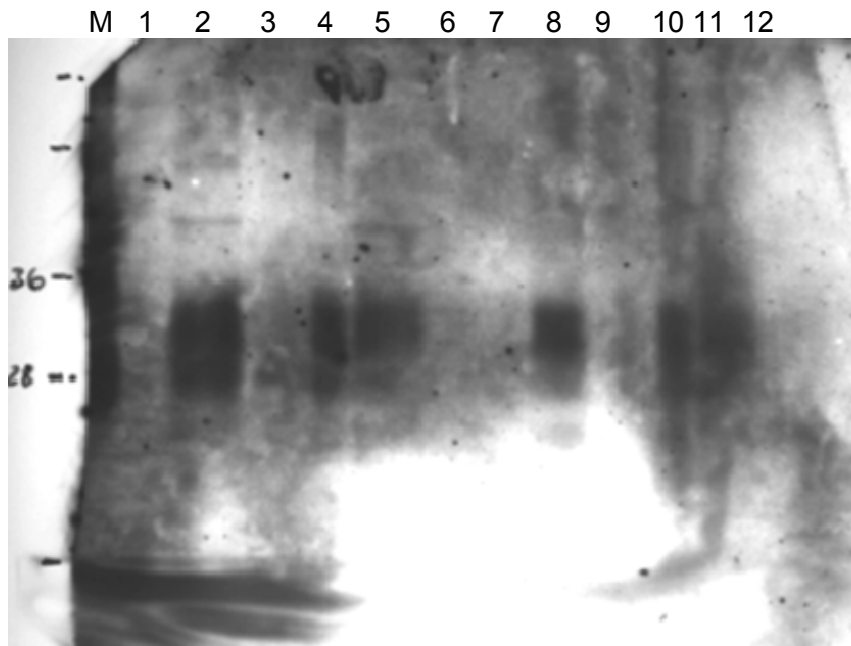
Figure 11: Western blot analysis of PTA precipitated PBMC fractions spiked with brain homogenate. Lane 1-3: 10^6 PBMCs spiked with negative brain homogenate (bh), pellet, supernatant, wash. Lane 4-6 PBMCs spiked with scrapie positive bh, pellet, supernatant, wash. Lane 7-9: negative spike only, lane 10-12 positive spike only, pellet, supernatant, wash.

d)   Brain tissue from cattle with clinical BSE

In order to adapt our method to BSE in cattle, we had to analyze brain material from BSE-infected animals as the first step in protocol development. First we optimised our pre-purification protocol using the PTA precipitation. PrP^{BSE} was precipitated in presence or absence of magnesium chloride. It should be noted that the detergent sarkosyl, routinely used during the brain homogenate preparation, becomes insoluble in the presence of magnesium ions and therefore might interfere with the precipitation of PrP aggregates. According to the protocol Wille et al. (2009) washing steps of pellets were performed with PTA-containing solution to avoid solubilization of aggregates.

We subjected all samples to western blot analysis (fig. 12). PrP^{BSE} content differs drastically between the 6 positive samples. Indeed, sample P6 yields only a faint signal that is barely detectable in the western blot, and could even be a spill-over from lane 5.
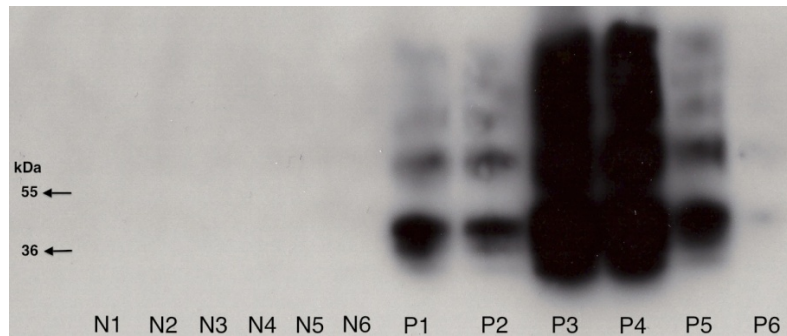
Figure 12: Western blot analysis of PrP^{BSE} pre-purified by PTA-precipitation of 6 BSE and 6 non-BSE brain homogenates. Antibody 3F4 was used for detection.

e) Cerebrospinal fluid from cattle with clinical BSE

Because initially no blood samples from BSE-infected cattle were available, we started using cerebrospinal fluid, however, from a very limited number of animals. Due to the very low content of PrP molecules in CSF we first considered measuring crude material without any pretreatment to avoid any loss of signal. Some control samples yield a strong signal probably due to interfering components in the crude material. Therefore we decided to prepurify the CSF samples in the same way we did for brain tissue using PTA-precipitation. The artifacts were absent in the PTA pretreated samples. Although in these very early experiments no differentiation between positive and negative samples was achieved by surface FIDA, false negatives were suppressed. Therefore, we decided in favor of PTA-pretreatment, since background signals were low. Next we adjusted our CSF samples to 2% sarkosyl. Pellets and supernatant resulting from 200 µl crude CSF as starting material of the PTA-precipitation were analysed in presence and absence of sarkosyl (fig. 12). We could not detect PrP in the samples by western blot analysis (data not shown), but in a denaturing PAGE, a significant purification effect can be seen comparing protein (not PrP) content of supernatant and pellet after silver staining.
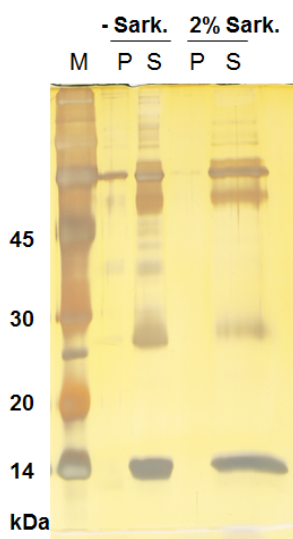
Fig. 13 Silver staining after PAGE of PTA-precipitated CSF. The precipitation was done either using 2% sarkosyl during precipitation and without sarkosyl. P. pellet, S: supernatant.

Introduction of a centrifugation step during target incubation

From earlier results it is obvious, that the variability of signals from the negative samples is still too high which prevents the identification of positive samples with low signals. To increase the signal-to-noise ratio we introduced a centrifugation step in the preparation protocol: After applying the target to the chip surface the plate is centrifuged at 1,000 g for 1 hour. This is beneficial for several reasons: i) the procedure is less time-consuming, since previously we incubated the sample overnight. ii) Binding of relatively large aggregates that diffuse slowly in solution is accelerated significantly. iii) Residual PrP^C monomers remain in the supernatant as they do not reach the surface within 1 hour of 1,000 g centrifugation. Figure 14 exemplifies the effect of the centrifugation step. Plasma from two scrapie-positive and two control animals was pre-purified by lipase treatment and PTA precipitation as described above. Pellets were resuspended, and incubated on the chip surface either with or without centrifugation. Although centrifugation causes a slightly higher background in the negative samples, signals from the positives are much higher than without centrifugation. In conclusion, signal-to-noise ratio is significantly improved when introducing this centrifugation step.

ΣI
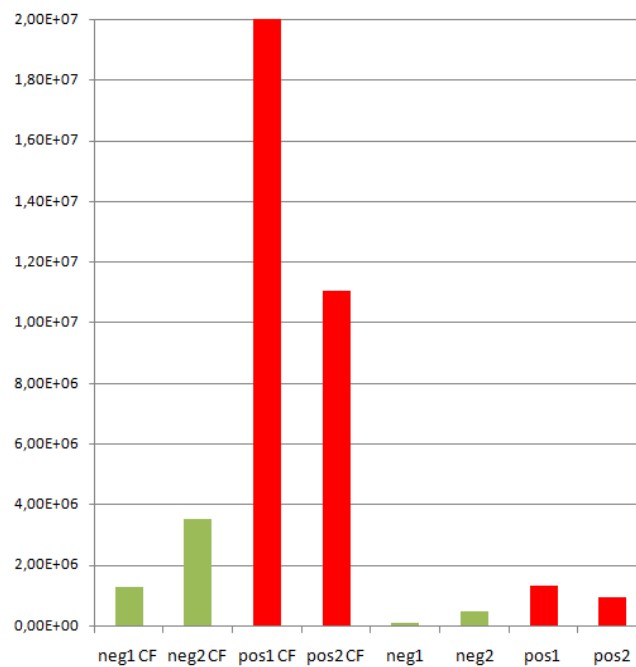
Figure 14. Target incubation on the chip surface with or without centrifugation.
Two positive and two negative sheep Scrapie plasma samples were incubated on the plate surface either with (CF) or without centrifugation. Aggregates were labelled with mAb Saf32 and L42. Images from the chip surface were background-corrected employing intensity cutoff. Images from both laser channels were colocalized, the remaining signals were summarized and displayed in a bar chart. Although background signals in the negative samples are elevated, centrifugation yields a significantly higher signal-to-noise ratio.

Replacement of scanning optics by imaging optics.

We tested a new instrumental development for particle counting by surface-FIDA. The optic was enhanced by a 3D-Piezo which is able to localise the fluorescence signal, thus enabling imaging. Therefore we are able to get images of the fluorescence intensity distribution, which enables the identification of particle size and shape as well as background artefacts.

Data processing

During the whole project we established and used different data processing methods. Most data shown were measured in the imaging surface FIDA mode and analysed by intensity evaluation. Therefore in this chapter we do not show original data, but explain our work on bioinformatics of the image processing and the measurement mode. We should point out that the biochemistry of sample preparation, the biophysics of setup and the bioinformatics of data processing are handled in iterative cycles, i.e. progress in one procedure allowed us to improve the consecutive steps.

Our assay is based on Dual-Color Fluorescence Correlation Spectroscopy (FCS). One has to explain that we do not apply the original correlation evaluation, i.e. correlation of diffusing particles, but we count fixed particles with varying intensity; correspondingly the method is called fluorescence intensity distribution analysis (FIDA). The instrument we are using was recently upgraded with an XY-scanning piezo unit. FIDA is recorded as a function of focus position and a scan of district in the well can thus be translated into an image in form of pixel intensities. We developed software capable of automatically analyzing a complete set of data. The following operations were applied to a series of images in a batch mode:

    i) The signals from both channels are normalized. This is necessary as signal output from both channels can differ significantly due to differences in laser excitation power, degree of labeling, antibody binding constants, and quantum yield of fluorescence dyes.

    ii) A fixed cutoff is subtracted from each pixel intensity value.

    iii) Images from both channels are tested for co-localization. Thereby, only particles such as PrP aggregates that yield signals in both channels are evaluated.

    iv) Finally, all colocalized particles are collected and analysed with respect to their sizes (number of pixels), their number, and their intensities (fig. 15).
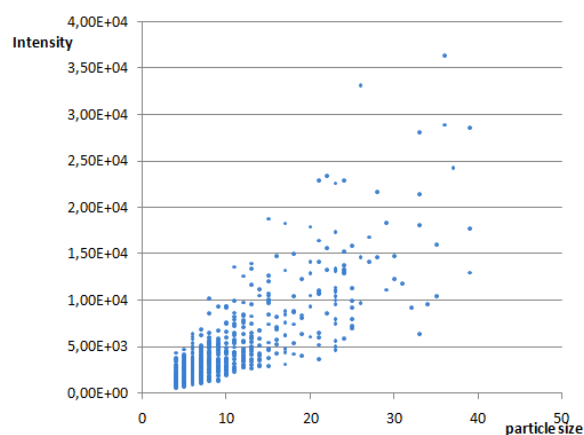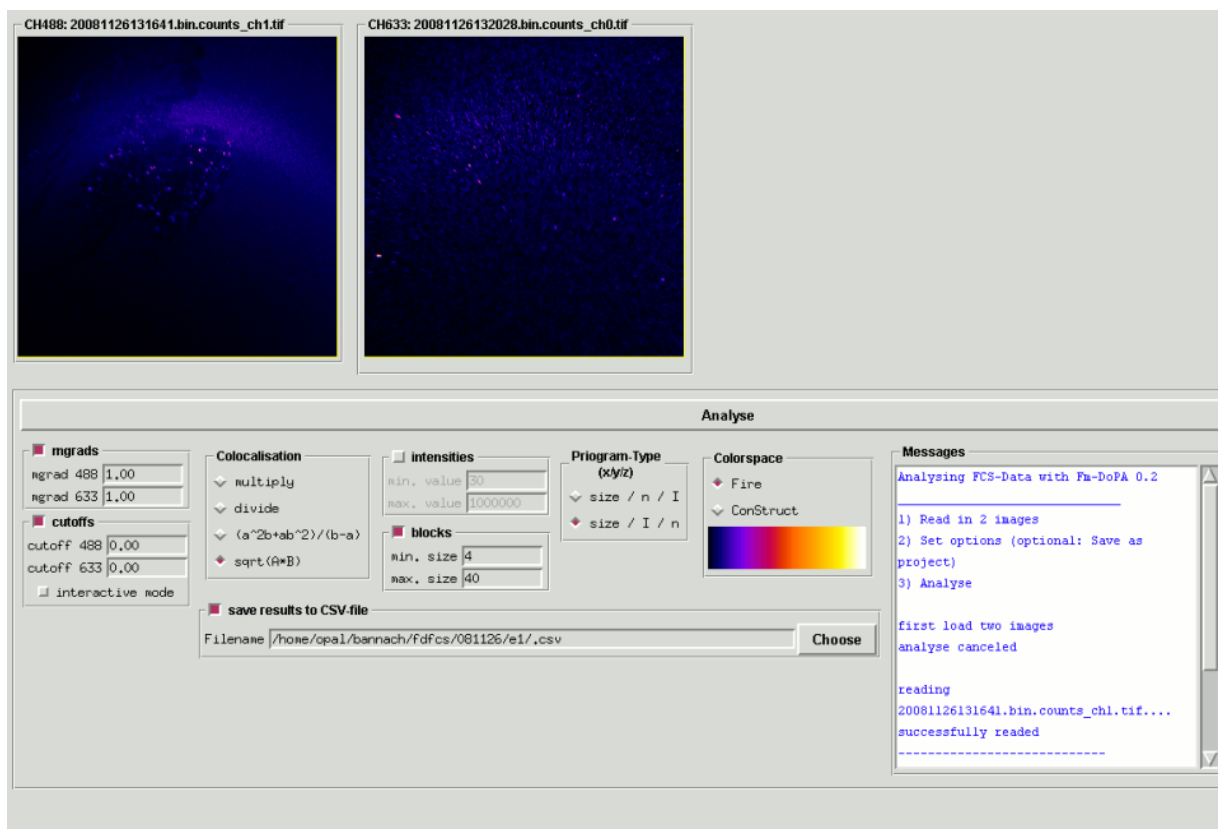
Fig. 15 Multiparameter particle analysis by image evaluation. A software tool was developed that automatically processes image data. Normalization by degree of labeling, subtraction of a cutoff value and colocalization was applied. Images were analysed with respect to particle number (number of blue dots), particle size (abscissa), and total particle intensities (ordinate).

We observed some instrumental artifacts, which are caused by laser light reflection and asymmetric illumination. These artifacts were only obtained when measuring near or directly on the surface. Therefore we first introduced new filter sets to reduce the reflected laser light. In a second step we introduced an algorithm to correct for continuous background changes in the data processing (fig. 15). The algorithm is based on the "rolling ball" algorithm (Sternberg 1983).

Channel 1

- background

x deg. lab.
- cutoff

colocalize

Image Analysis

Channel 2
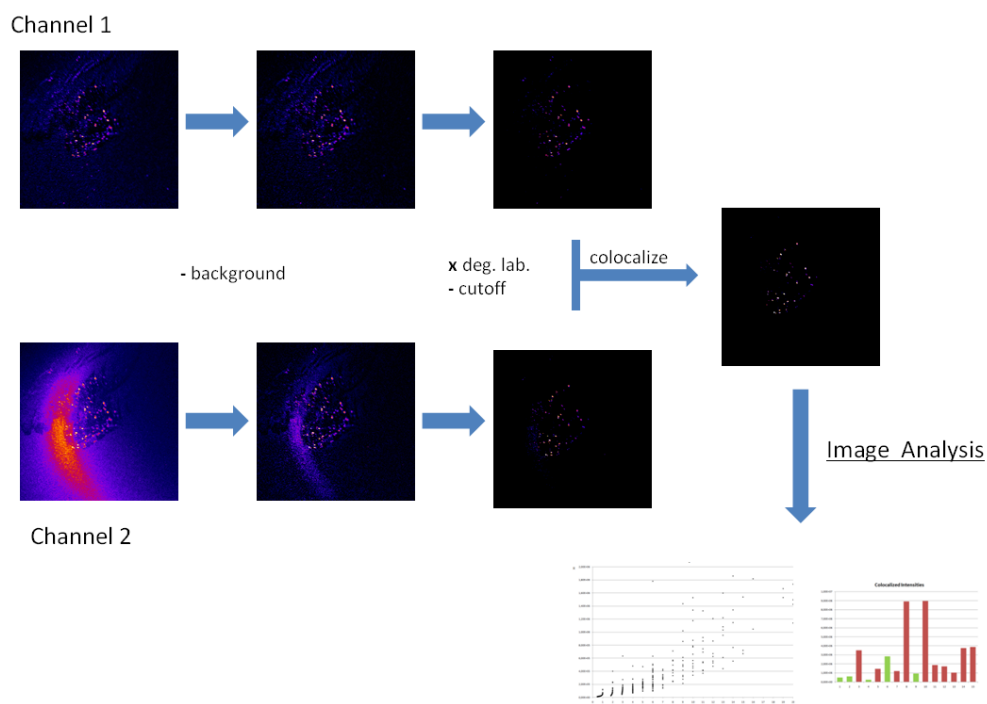
Fig. 15 Reduction of artificial background by image processing algorithm

Two different processes of data processing were applied which are described in the following in some detail:

Procedure 1

Improved background removal and Intensity evaluation

Efficient reduction of background signals is crucial to differentiate positive from negative samples. Background reduction can be achieved both by optimised experimental procedures and image data processing. As previously shown, more stringent washing conditions, e.g. application of low concentrations of SDS, do not only lead to lower background, but also may deplete or even abolish positive signals. Therefore we also focused on a posteriori background removal via image data processing.

The "subtract background" function in the open source ImageJ tool employs the so called 'rolling ball' algorithm (Sternberg 1983). This algorithm does not only compensate uneven intensity distribution within an individual image, but is also capable to select for particular particle sizes. The image data can be visualized as a 3D surface with the pixel intensity values of the image being the height. A ball of a particular diameter selected as a parameter is roling over the back side of the surface. It can invade in peaks of larger diameter but not into those of smaller. Thereby it creates a background distribution, which is subsequently subtracted from the image. As a general rule, the smaller the ball radius, the more background is removed.

After 'rolling ball' background reduction an intensity cut-off was applied to a recorded image series from plasma samples. Figure 16 A shows an intensity evaluation after

cut-off application only, which still gives signals in a control sample A6, which is higher than a positive sample, e.g. A7. By executing an additional 'rolling ball' background subtraction (ball radius = 2 pixels), background noise from all negative samples could be efficiently suppressed (fig 16 B), entailing a drastic gain of sensitivity of the analysis. Moreover, from these analyses it became evident that relatively small but relatively bright particles are characteristic for the positive samples. We have to point out clearly that this optimization was only possible on samples with known identity. However, we also aim to apply the image processing steps described above on a panel of coded samples. In the evaluation of fig. 16 only signals of one fluorescence channel was taken into account.

A

B
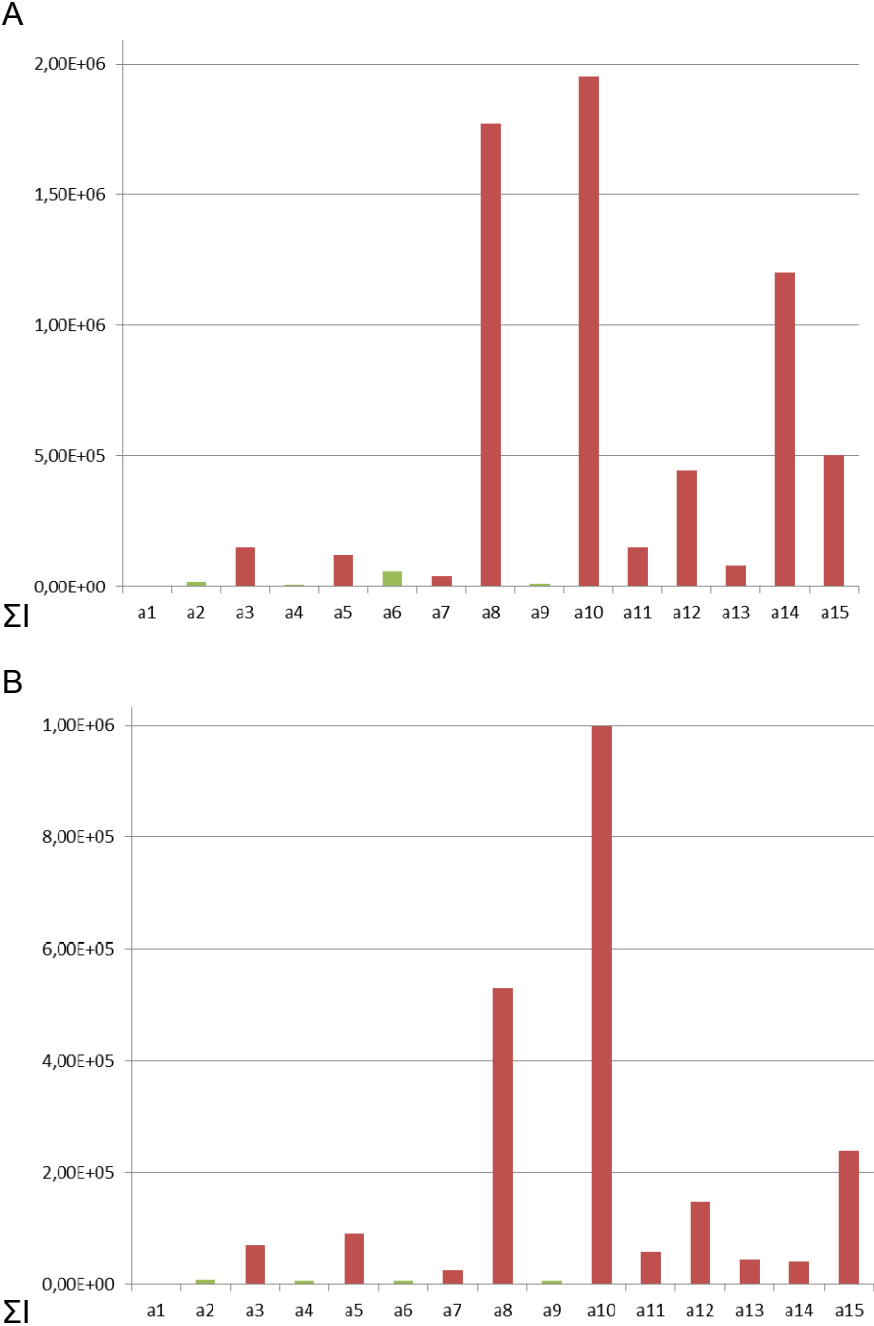
Fig 16 Comparison of former performed A and advanced intensity analysis B
Background signals could be reduced in samples a2 and a6

Procedure 2:

Support Vector Machine algorithm

Additional image parameters like particle size and colocalization of data from both fluorescence channels can be incorporated in the analysis. The classification model established here is based on the concept of the Support Vector Machine (SVM) algorithm. The work flow starts with the processing of images obtained from the surface-FIDA assay. The image data are converted into numerical data series particularly suitable for the SVM format. Using a suitable kernel function, cross-validation is performed to determine the best parameters distinguishing the images from Scrapie and control samples. The model is trained to find the best parameters. The algorithm used is a learning technique for classification which is deterministic and interpretable. The modeling approach includes the stages as follows:

Stage 1: Image Processing

In the first stage the images obtained from surface-FIDA are processed. The ImageJ tool is used for this purpose. The images are converted into 8 bit images where a maximum of 256 grey scales are represented at once. Images are thresholded to remove the background. Here an exponential function is applied both to remove background and enhance bright pixels, respectively.

Stage 2: Image Analysis

The processed images are analysed for data extraction, signal processing and determination of distinguishing parameters. The fluorescence images are obtained from two different channels, i.e.at wavelengths 488 nm and 633 nm. Images from these two wavelengths are colocalized using the ImageJ built-in colocalization plug-in "Colocalization Finder". Three parameters, i.e. signal number, size and Pearson's coefficient for co-localisation are used for model building.

Stage 3: Model Building

Here the classification model is built using the SVM algorithm.

The SVM classifier tool is used for this purpose. The data generated are divided into 2 subsets, a training and a test set. The model is trained using the training set. In figure 17 the advantage of using 3 parameter leading to a hyperplane over only 2 parameters is shown. The separating hyperplane differentiates more clearly in 3 dimensions compared to separating two areas in 2 distances. Extension to 4 parameters can be introduced.

In summary, SVM is a supervised learning method and classifies data by analyzing and recognizing subtle patterns in data. A hyperplane is built which is the decision plane dividing the data into 2 classes.
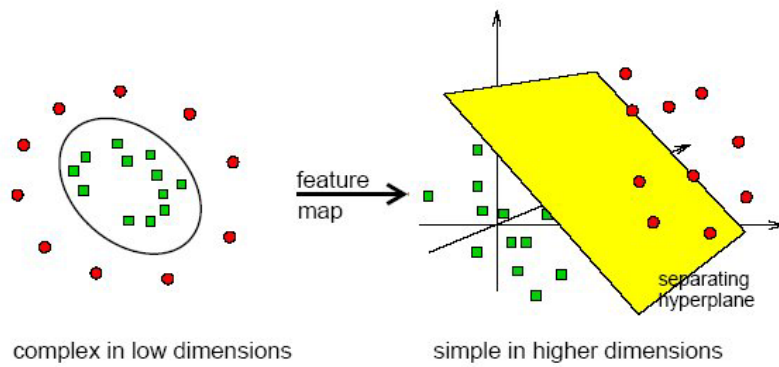
Figure 17 SVM: advantage of using 3 parameter over only 2 parameters
http://www.dtreg.com/svm.htm

Stage 4: Model Analysis

After the model has been built, it is applied to the blinded data to check for the accuracy of the model. Different combinations of parameters are applied to determine the level of accuracy. The level of accuracy is then checked for by comparing the computerized results with the in-vitro results.

Application of optimised surface-FIDA to different tissues and body fluids from various species

    a)   **Brain tissue from sheep with clinical Scrapie**

In order to show that the principle of our assay works, we subjected PTA-purified Scrapie brain material to surface-FIDA analysis. As depicted in figure 18 we were able to differentiate diseased from healthy controls. However, the negative samples gave also rise to non-specific signals, complicating a statistical evaluation of antibody binding performance.
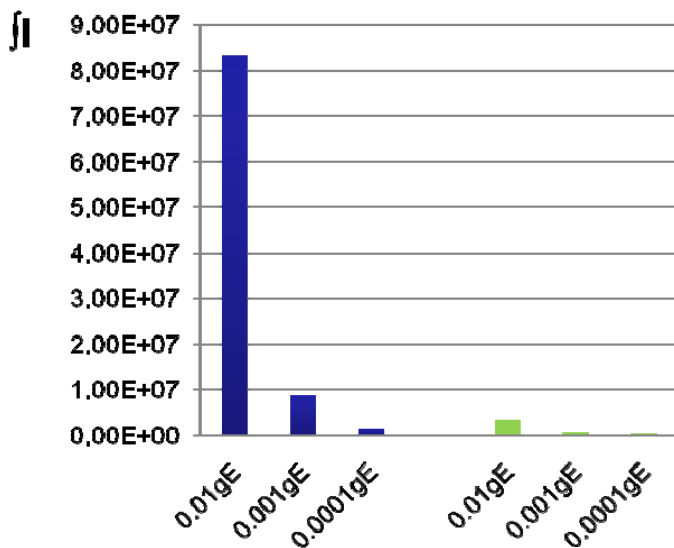
Fig 18:
Dilution of PrP^{Sc} purified from Scrapie brain homogenate in the surface-FIDA assay, blue infected, green: not infected; gE: gram equivalent. The details of FIDA analysis will be outlined below.

26

Because the analysis of PrP^{Sc} from brain homogenate of sheep was not the target of the project, we decided to utilize for further method optimization aggregated sheep recPrP for spiking of ovine plasma. Moreover, this approach can provide valuable information concerning the expected background signals from the negative plasma samples as well as the affinity of the antibodies to aggregated sheep PrP.

b)   PBMC fractions from sheep with clinical scrapie

Lipase treatment was also introduced to the PBMC preparation in order to avoid coverage of PrP epitopes by lipids and lipoproteins. This effect is clearly seen in fig 19 .
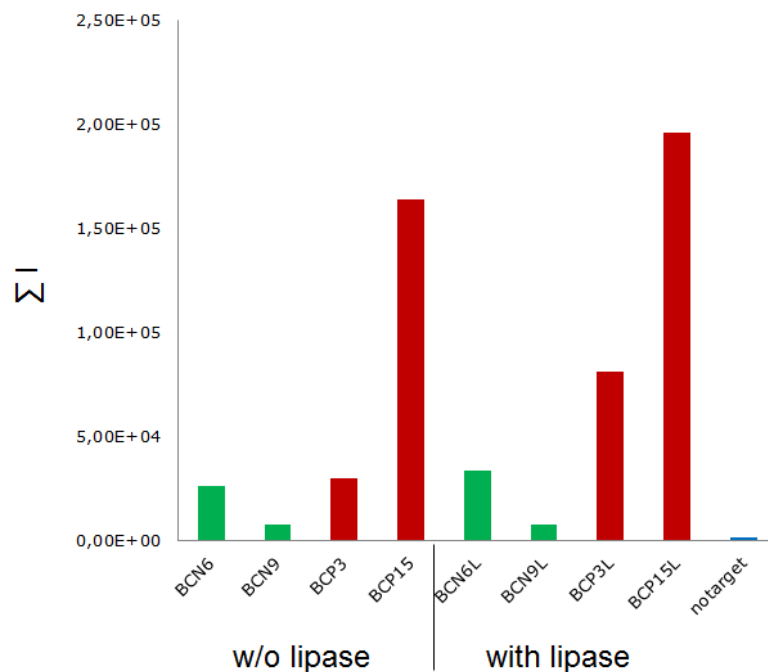
Figure 19. Effect of lipase treatment. Two negative (green) and two scrapie-positive (red) PBMC (10^6 cells) samples were treated either with or without lipase, and subsequently subjected to surface FIDA analysis.

Whereas in former measurements preparation was carried out on larger series of samples in parallel (up to 15 samples, five are shown in fig. 20), we processed now only up to 5 samples in parallel. In this way we could guarantee much better highly reproducible, i.e. constant incubation times of precipitation, incubation and washing. The risk of losing a pellet after precipitation and washing or not washing was reduced reproducibly.

Washing the chip with 0.2% SDS was found previously very useful when applied to brain homogenate. In PBMC samples, however, this washing step was skipped,

because any loss of signal has to be avoided. The results show now clear distinction between negative and positive samples; negative samples 1 and 2 are now reproducibly low, the positive sample 8 (lost in fig. 20A) shows now a high signal (Fig 20B). Negative samples are close to the buffer signal. We could not always use the same samples for our optimization series because the size of samples is limited.
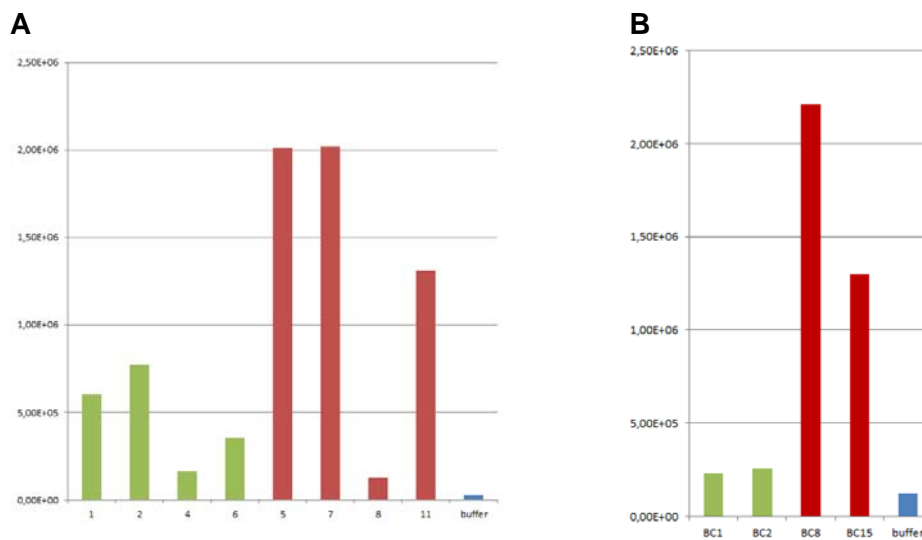
Figure 20: Surface-FIDA of PBMC samples. A) Results from a larger series of samples of negative (green) and positive (red) scrapie PBMC cases. Sample 8 (positive) was probably lost and samples 1 & 2 (negative) are too high due to background issues. B) Two negative and two positive (clinical) sheep were subjected to FIDA analysis..

c)   **Blood plasma from sheep with clinical scrapie**

For serial measurements, Dr. Linda Terry, VLA kindly provided us blinded sheep plasma samples. We prepared, measured and analysed the data of the plasma samples as described above. We then obtained the correlation of the samples to infected and healthy sheep (fig. 21).
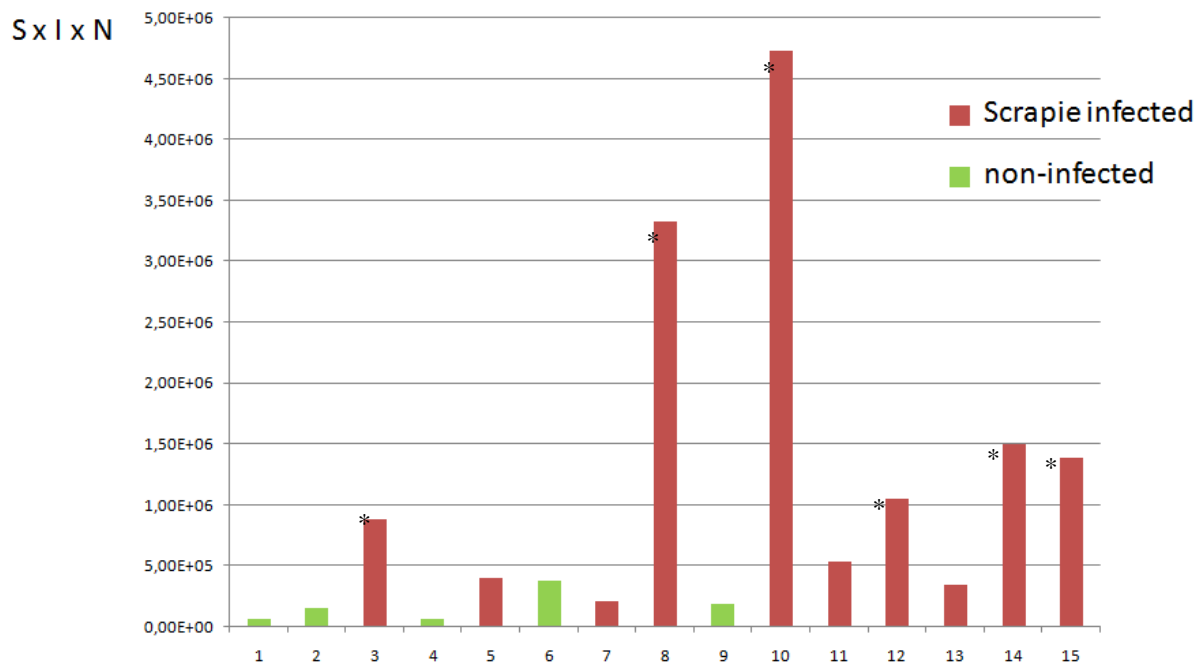
Fig. 21 Serial measurement of sheep plasma
When samples were still blinded, we estimated a border line at 5.00 E+05 and those marked an asterisk were classified as positive. After unblinding samples from Scrapie infected sheep are shown in red; samples from healthy sheep are presented in green.

The data shown in fig. 21 are based on a 1D analysis i.e. applying only one detection antibody. Within our experiments we obtained good results using different detection antibodies in 1D analysis. The results were obtained using Saf32. The epitope of Saf32 is located in the N-terminus, precisely within the octarepeat region. This means that there are eight epitopes on the prion protein for Saf32 recognition, which explains the remarkable 1D performance of this antibody.

Using only Saf32 we could show clear tendencies to differentiate between plasma samples of Scrapie-infected sheep from healthy controls. If the signals were about or more than twice as high as the series of low signal samples it was valued as positive sample. The border line was estimated around 5.00 E+5.

In our experiments we found out that two different antibodies, e.g. Saf 32 and FH11, worked well when used separately in 1D experiments. However, when both antibodies are incubated simultaneously, Saf32 suppresses the signal of FH11, most probably because FH11 binds also to the N-terminal part. Therefore in the following experiments we only considered those antibodies specific for the C-terminal part – like L42 -, or a structure specific antibody. Furthermore, freezing and thawing of plasma samples leads to artefacts. Therefore, we have to divide the samples into aliquots before freezing. In summary, the results showed the proof of principle, that we are able to detect prion protein particles in the plasma fraction of sheep blood.

After unblinding the samples by our colleagues in Weybridge, we realized that we could identify 6 out of 10 scrapie-positive, clinical animals without any false-positives. Recently Terry et al. (2009) published a study applying an improved ELISA test, in which the authors could detect PrP^{Sc} in PBMCs from 55% of scrapie-infected sheep. Fortunately, they had used the same samples as available to us, and not only the total sensitivity of 55-60%, but also the 60% detected cases were more or less the same. It should be noted, however, that infectivity in the PBMC fraction is about one order of magnitude higher compared to blood plasma. Terry et al. reported that they were not able to detect PrP^{Sc} in the plasma of those samples. Therefore, it was obvious for us to apply our method to PBMC and achieve thereby a higher sensitivity.

We determined the size distribution of particles of a Scrapie sample and a negative control (Fig. 22). Whereas in both samples small sizes are present (below 10 pixels), large sizes are mainly present in the Scrapie sample. Characteristic sizes of 8 – 20 pixels correlate with a rolling ball radius around 2 pixels.
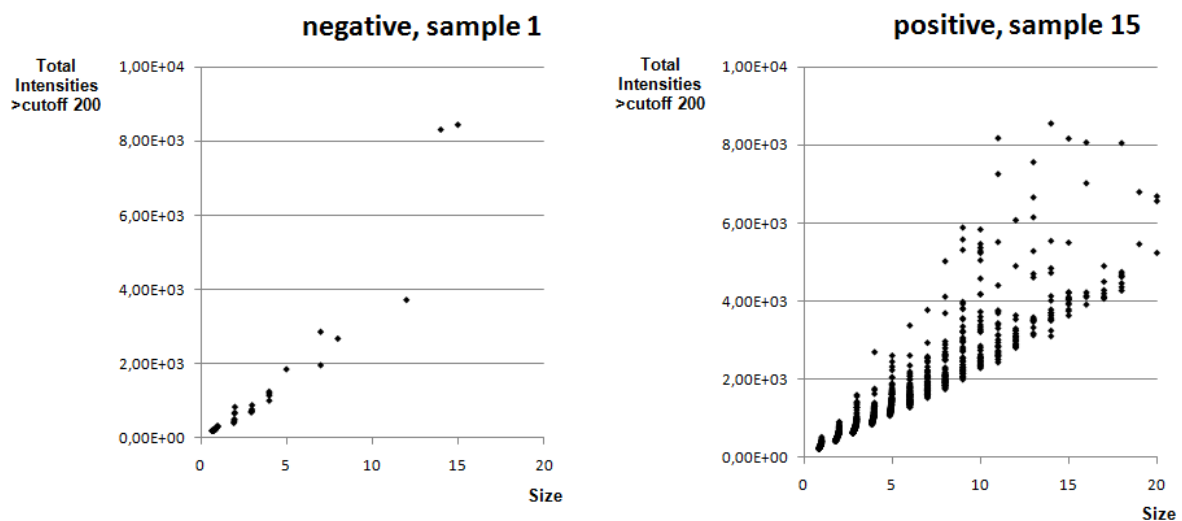
Fig. 22 Detailed multi-parameter evaluation of a negative and a positive sample. Every dot represents one particle.

However, when trying to reproduce our initial experiments we encountered some adversities, i.e. artifacts in our surface-FIDA method that were most probably due to repeated freezing and thawing of samples. Therefore we requested another set of fresh plasma samples (blinded) from the VLA. With these new samples we could reproduce our results in terms of sensitivity. As before, we were able to identify 6 out of 10 Scrapie-positive sheep (figure 23).

ΣI
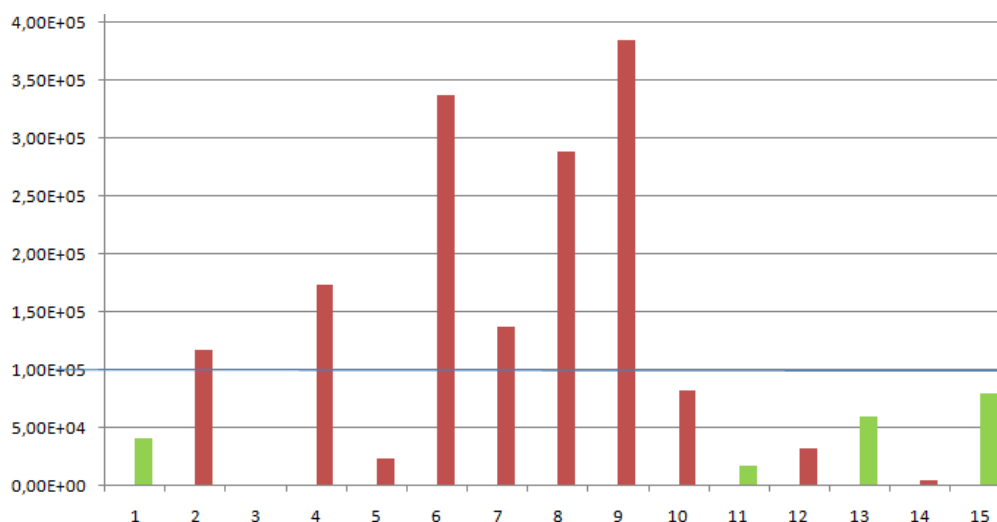
Figure 23: Reproduction of the analysis of a set of blinded plasma samples.
Blood plasma from 10 clinical and 5 control sheep was subjected to surface-FIDA analysis employing Saf32 as capture and probe1, and L42 as probe2. 6 out of 10 scrapie-positive animals were identified, which matches our earlier finding.

Determination of the sensitivity limit in correlation with the state of disease using scrapie plasma samples

For determination of the detection limit, first we considered spiking experiments employing either PrP^{Sc} from brain homogenate or recombinant PrP as the source of choice. In initial experiments, PTA-prepurified or crude brain homogenate turned out to be not suited as spiking material. Brain homogenate was introduced in a plasma sample led to irreproducible results. Consequently we focused directly on plasma preparation instead of using brain homogenate purification. Although recombinant PrP was used for optimization of other steps it is not ideal for serial dilution experiments, as the aggregation state and structural features might probably not reflect the *in vivo* properties of Scrapie prions in sheep plasma.

The amount of PrP^{Sc} in blood fractions depends on the time after inoculation and does not increase monotonically after inoculation. According to infection studies it was found to be even higher in some samples in the preclinical state of the disease than in the clinical state (personal information of J.P. Deslys). Consequently, determination of the detection limit with spiking material in blood of sheep might yield artificial results, and it is more appropriate to determine the detection limit directly in blood samples of Scrapie sheep at different time periods after inoculation.

Analysis of blinded plasma samples from sheep
From the VLA Biological Archive we obtained a panel of coded plasma samples, including sequential bleeds from scrapie-exposed animals in the pre-clinical state, *post mortem* samples, as well as negative plasma samples from scrapie-free sheep.

We received a total of 75 aliquots à 1 ml. Preparation and measurement of a maximum of 8 samples was performed on 10 different days. On each day, we also processed and analysed the standard samples with known identity as described above, including buffer control, pooled Scrapie-negative plasma, and pooled Scrapie-positive plasma.

We faced some instrumental problems during the serial measurements. Aligning the height of the focus on top of the surface did work optimally, and the instrument carrying out that correction automatically was not available in our safety containment. Visual inspection of the obtained images indicated some variations in sample quality, since some samples exhibited obvious image artefacts. Prior to evaluation we had to exclude those strongly artificial images. On some plates, performance of standard samples was poor, i.e. positive samples could not be differentiated from control samples. Therefore, we considered all blinded samples which were prepared and measured in parallel with these standards as not determinable. Also the samples as delivered show different consistency: some had impurities and products from haemolysis.

Evaluation and classification was carried out by two different approaches as described above: i) Images were background reduced, and remaining intensities were summed up. Samples above an intensity threshold from negative controls were considered positive. ii) Using a supervised learning algorithm, a model is trained with image information from the standard samples. This model is then applied to the blinded samples for classification as either negative or positive. Table 1 summarizes the results of classification.

Table 1: Classification of coded plasma samples. Blinded samples were either classified according to the remaining intensity after background removal, or via an SVM-based approach (multiparameter). pos/neg (intensity evaluation): positive but close to background. pos/neg (multiparameter evaluation): depends critically on the choice of parameters. Due to poor performance of standard samples, plates f,g,h,j were not evaluated. nd: not determinable. PG#: animal ID-number. PM: *post mortem* sample

Well	Sample ID	Intensity	Multiparameter	Result
d5	bag14	nd	nd	PG0816/09, 2nd Bleed
d6	bag57	negative	negative	PG0816/09, 3rd Bleed
d7	bag70	negative	negative	PG0816/09, 3rd Bleed
d8	bag75	pos/neg	pos/neg	PG0816/09, PM
d9	bag23	negative	negative	PG0818/09, PM
d10	bag32	positive	positive	PG0818/09, 3rd Bleed
d11	bag45	positive	pos/neg	PG0818/09, 3rd Bleed
d12	bag63	positive	positive	PG0818/09, 3rd Bleed
e5	bag24	positive	negative	PG0818/09, 1st Bleed
e6	bag28	positive	negative	PG0818/09, 2nd Bleed
e7	bag44	negative	pos/neg	PG0818/09, 1st Bleed
e8	bag53	positive	pos/neg	PG0818/09, 1st Bleed
e9	bag22	negative	pos/neg	PG0817/09, 1st Bleed
e10	bag52	negative	pos/neg	PG0816/09, 4th Bleed
e11	bag66	positive	positive	PG0816/09, 2nd Bleed
e12	bag78	pos/neg	pos/neg	PG0816/09, 4th Bleed
i5	bag13	negative	negative	PG 0957 / 06, negative
i6	bag27	negative	pos/neg	PG 0972 / 08, negative
i7	bag26	negative	negative	PG 0461 / 03, negative
i8	bag31	nd	nd	PG 1233 / 05, negative
i9	bag47	negative	positive	PG 1124 / 06, negative
i10	bag58	nd	nd	PG 1233 / 05, negative
i11	bag64	negative	positive	PG 0673 / 08, negative
i12	bag79	negative	pos/neg	PG 1113 / 05, negative
k5	bag11	positive	negative	PG 623 / 05, negative
k6	bag25	negative	negative	PG0593/09, 4th Bleed
k7	bag39	pos/neg	positive	PG0593/09, 3rd Bleed
k8	bag43	pos/neg	positive	PG 0503 / 06, negative
k9	bag51	negative	negative	PG 0957 / 06, negative
k10	bag65	pos/neg	positive	PG0593/09, 4th Bleed
k11	bag73	negative	negative	PG0593/09, 3rd Bleed
k12	bag76	negative	negative	PG 0673 / 08, negative
l5	bag20	negative	negative	PG0593/09, 2nd Bleed

l6	bag36	negative	negative	PG0593/09, PM
l7	bag46	negative	negative	PG0593/09, 3rd Bleed
l8	bag55	positive	pos/neg	PG0593/09, 2nd Bleed
l9	bag74	negative	negative	PG0593/09, 2nd Bleed
l10	bag81	negative	negative	PG0593/09, 4th Bleed
l11	bag82	positive	negative	PG0593/09, 1st Bleed
l12	bag84	negative	negative	PG0593/09, PM
m5	bag30	positive	positive	PG0593/09, 1st Bleed
m6	bag37	positive	positive	PG0593/09, 1st Bleed
m7	bag40	negative	positive	PG0593/09, PM

We sent these results to VLA Biological Archive. After decoding we aligned the samples to the disease state.

Based on the present results from the decoding (cf. Table 1, results), we are not convinced that our method is capable to diagnose individual animals according to the state of the disease. We have a lot of indications that our device was in a bad condition, which we could realize only after measurements. We applied for a new device, but the decision is not jet made if and/or when we might get one. However, since we identified some pre-clinical animals as scrapie-positive, it might well be that pre-clinical blood generally harbours more prion aggregates than clinical plasma.

d) Brain tissue from cattle with clinical BSE

When analyzing samples from BSE-afflicted cattle most of the optimization could be transferred from sheep samples. The PTA precipitation was adopted using brain homogenate. As can be seen in figure 24, avoidance of magnesium chloride results in a significant gain of signal in BSE-positive samples, compared to samples precipitated in the presence of magnesium, whereas background signal from the negative brain is elevated only slightly.
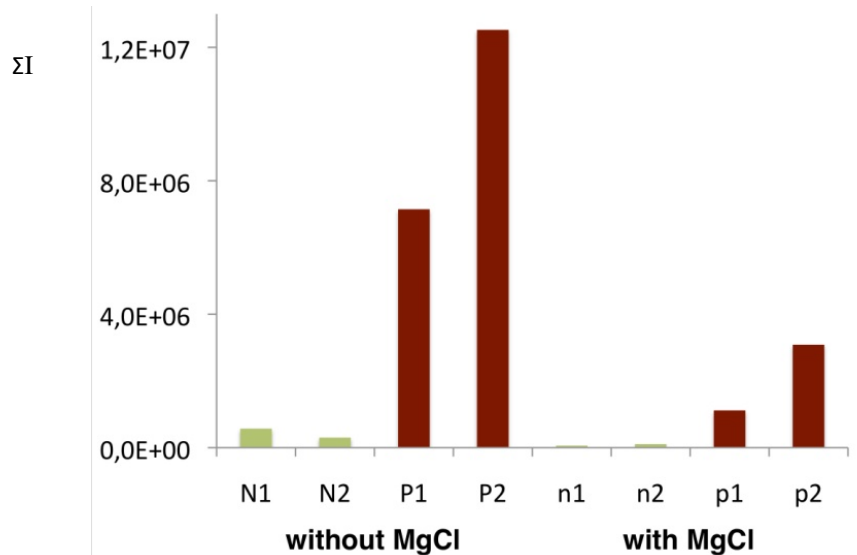
Figure 24: Influence of MgCl$_2$ on the precipitation of prion particles from brain homogenate by PTA as analysed by surface-FIDA. Two BSE-positive (P1, P2) and two control (N1, N2) samples were measured. Saf32 was used as capture and probe. The fluorescence intensities above a cut-off 100 were summed up.

Having optimised the purification protocol we performed a serial measurement of brain homogenate from six BSE-afflicted and six control animals. As shown in figure 25, we could clearly identify 5 out of 6 positive animals by surface FIDA. The absence of signal in sample P6 might result from a very low PrP^{BSE} titer in this animal. Therefore we subjected all samples to western blot analysis. As already became evident from surface-FIDA analysis, PrP^{BSE} content differs drastically within the 6 positive samples. Moreover signal variations match precisely between surface-FIDA and western blot analysis.
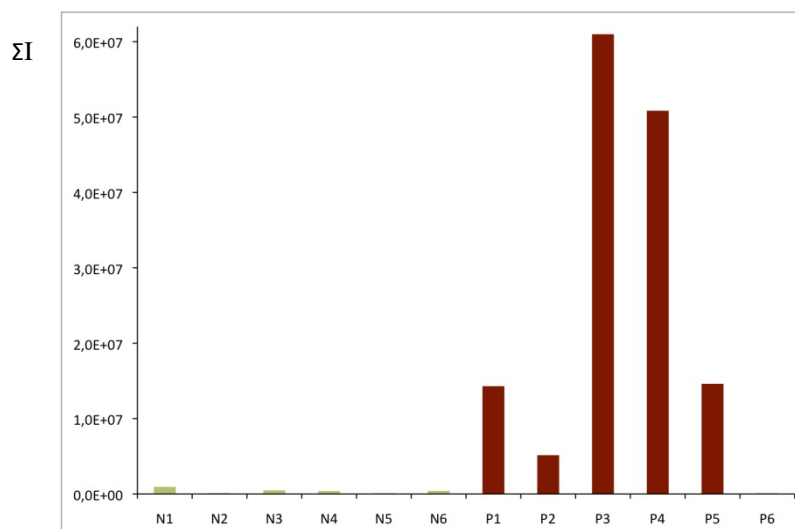
Figure 25: Surface-FIDA of purified brain homogenate of BSE-infected and healthy cattle. SAF-32 was used as capture and probe. The fluorescence intensities of one channel above a cut-off 100 were summed up.

Cerebrospinal fluid (CSF) from BSE-afflicted cattle

Because we had no blood samples from BSE infected cattle, we started using CSF, however, from very limited sample numbers. CSF was previously shown to contain PrP aggregates (Birkmann et al. 2006). We are aware that analysis of CSF from cattle is of low applicational value, but we regard it as a step in procedural development from brain homogenate to blood fractions. Due to the very low content of PrP molecules in CSF we first considered measuring crude material without any pretreatment to avoid any loss of signal. Surprisingly control sample N1 yields a strong signal probably due to interfering components in the crude material. Figure 26 shows a comparison of crude CSF *versus* CSF that was treated with PTA. These serious artifacts were absent in the PTA pretreated samples (fig. 26). Although in these very early experiments no differentiation between positive and negative samples was achieved, false negatives were suppressed. Therefore, we decided in favor of PTA-pretreatment, since background signals were low.
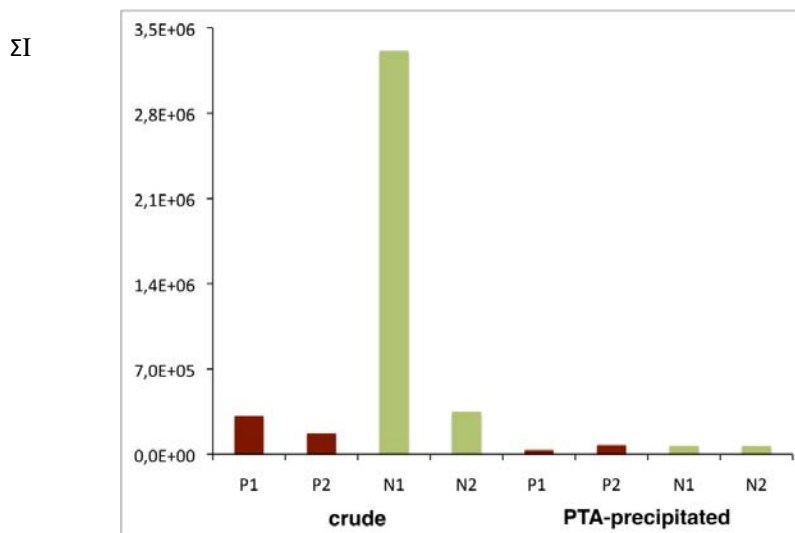
Figure 26: Surface FIDA of crude and PTA-precipitated CSF from cattle. CSF from 2 BSE positive (P1, P2) and 2 negative (N1, N2) samples was analysed. Saf32 was used as capture and probe. The fluorescence intensities of one channel above a cut-off 50 were summed up.

Next we adjusted our CSF samples to 2% sarkosyl. The effect of this treatment is exemplified in figure 27. As observed before, total fluorescent signal was extremely low in all samples. However, sample P2 exhibited a value that was significant higher compared to the other samples. These results are in line with the results we observed before, that we can detect PrP-particles in some but not in all CSF samples.

Finally we analysed 4 positive and 4 negative CSF samples in a serial measurement. Although the samples with the two highest signals were both BSE-positive, differences to signals from the other samples were non-significant. We did not continue to analyze CSF samples from cattle.
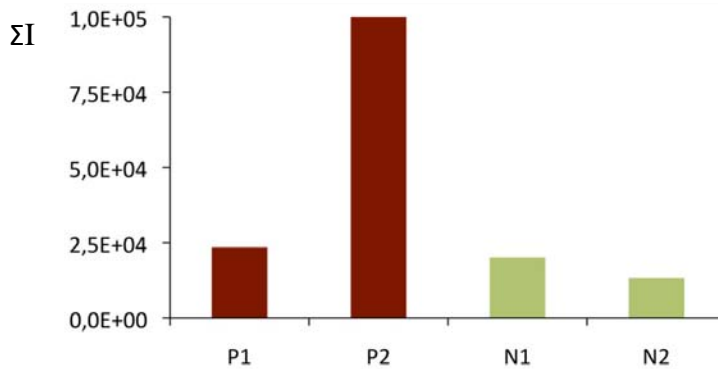
Figure 27: Surface-FIDA from CSF pretreated with sarkosyl. 2 BSE positive (P1, P2) and 2 negative (N1, N2) CSF samples were adjusted to 2% sarkosyl and precipitated with 2% PTA. Saf32 was used as capture and probe. The fluorescence intensities of one channel above a cut-off 50 were summed up.

Blood plasma from BSE-afflicted cattle

The situation with BSE in cattle is very similar to Scrapie in sheep in the sense that realistic detection limits have to be determined with natural sample in dependence upon the state of the disease instead of artificial spiking experiments.

We analysed blood samples from BSE-infected cattle but could not find prion particles by surface FIDA (fig. 28).

A

B

L42 alexa 633

Saf 32 alexa 488
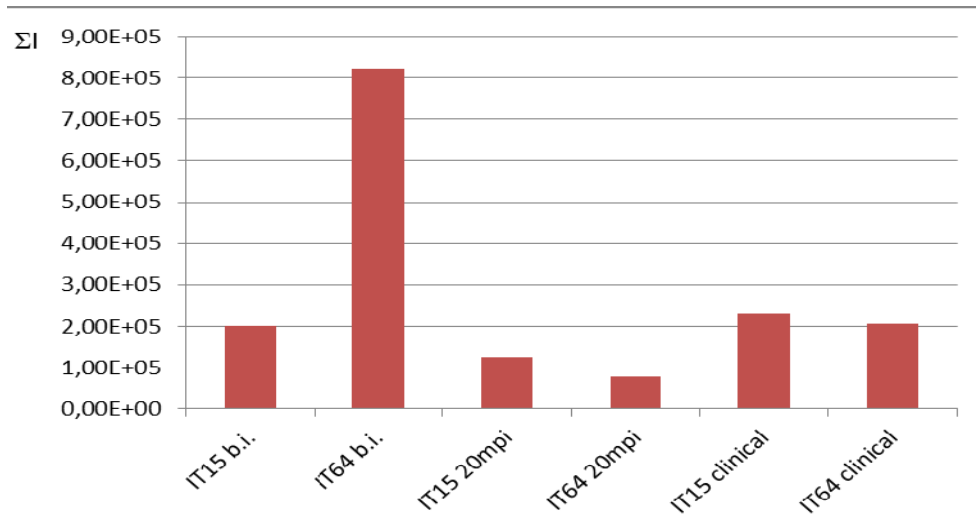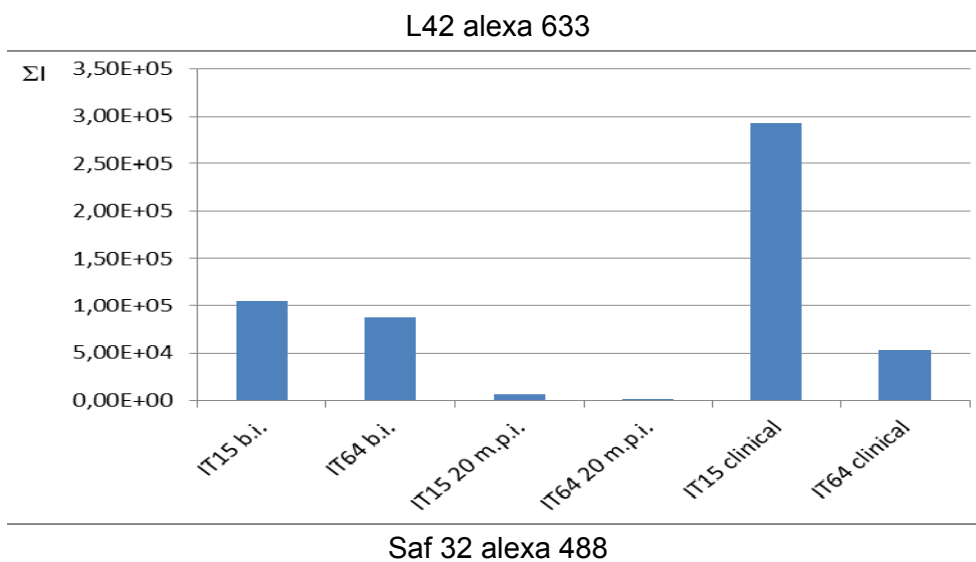
Figure 28: **Analysis of cattle plasma.** Plasma from two BSE-infected animals (IT15 and IT64) was obtained before inoculation (b.i.), at 20 month post inoculation (m.p.i.), and after the outbreak of clinical symptoms. Samples were prepurified as described above and subjected to surface FIDA. Background reduced images were analysed with respect to total fluorescence intensity.

From our results we argue, that there are no prion particles in blood plasma of BSE-infected cattle, which fits to the fact that infectivity in cattle blood has never been reported (World Health Organization, 2010). Furthermore, bioassays with bovine-transgenic mice demonstrated, that spleen and other lymphatic tissues from BSE-afflicted cattle are free of detectable infectivity (Buschmann and Groschup 2005).

Determination of the sensitivity limit in correlation with the state of disease for BSE samples from brain homogenate

In order to assess the sensitivity limit of our method in correlation with the stage of disease, we analysed brain samples of a first series from a pathogenesis study conducted by Dr. Groschup (Friederich Loeffler Institute, Isle of Riems). Calves had been orally challenged with BSE inoculum and were sacrificed 1, 4 and 8 months after infection. We prepared 5% brain homogenate from these samples, and compared them with samples from clinical and control animals by surface-FIDA (figure 29). As expected, signals from the clinical samples yielded the highest signal. However, the pre-clinical samples could not be differentiated from the controls. Since development of symptoms can take up to 40 months and more, analysed time points might be too early.
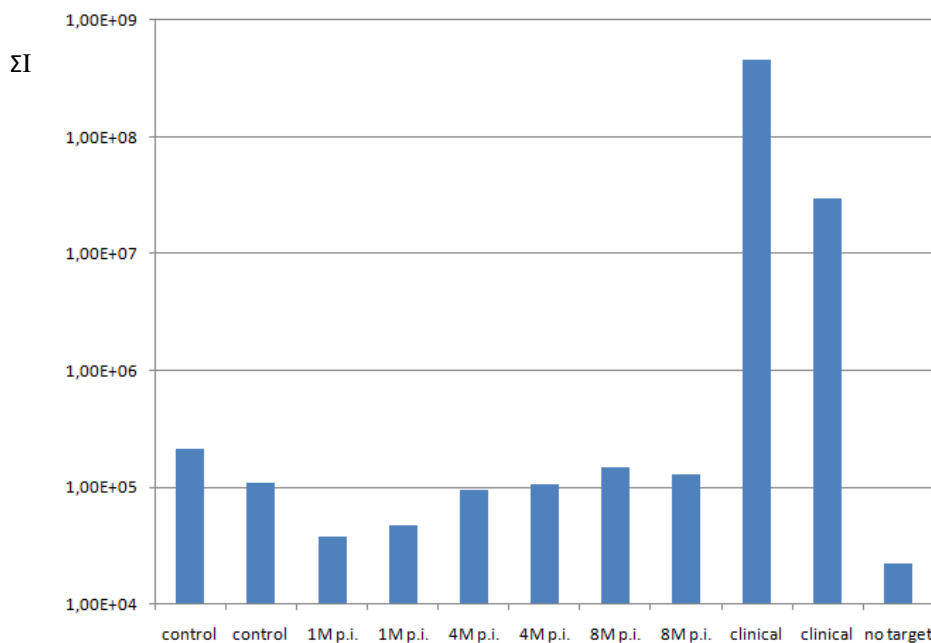
Figure 29: Analysis of a first series of BSE-samples from a pathogenesis study. Cattle were experimentally challenged with BSE inoculum. Individual animals were killed after 1, 4, and 8 months *post inoculum*. Intensities from the clinical samples were much higher compared to the preclinical samples. For clarity, the sum of intensity was therefore plotted on a logarithmic scale. 1D analysis with mAb Saf32.

Therefore we requested additional samples at later time points, and completed the series. Fig. 30 shows that we could identify two preclinical animals at 16 and 24 months post inoculation.
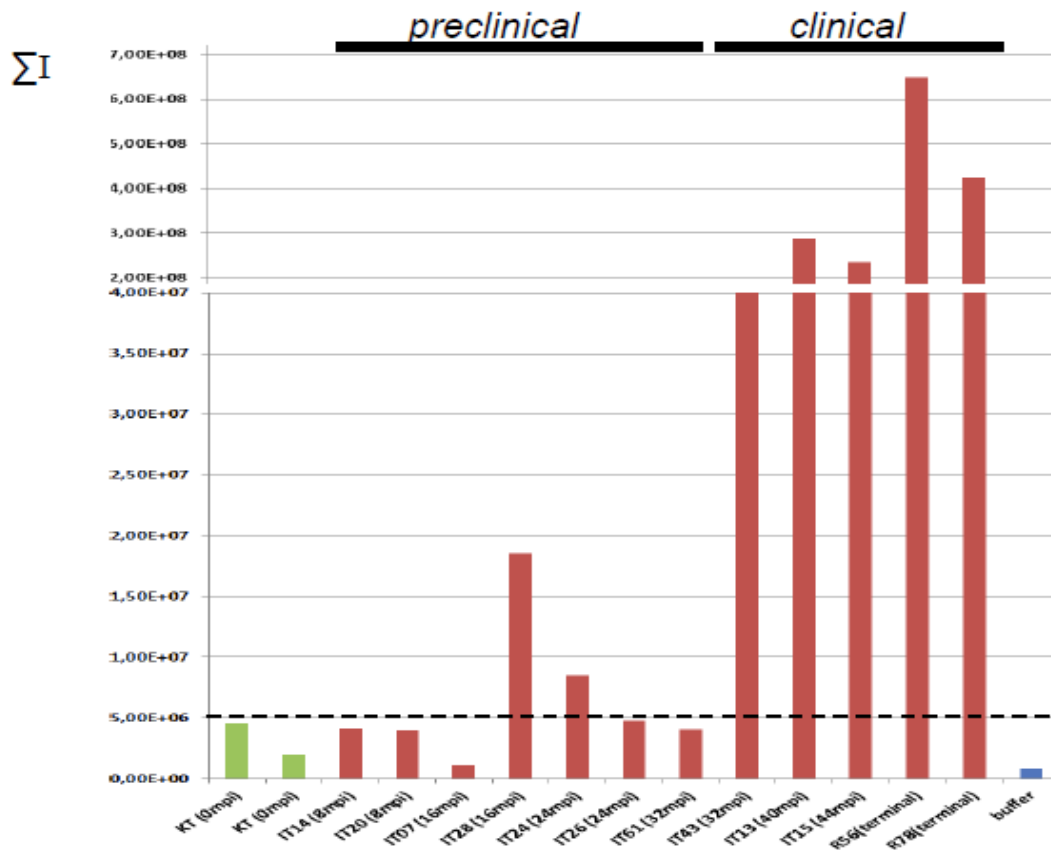
Figure 30: Analysis of the second series of BSE-samples from a pathogenesis study. Cattle were experimentally challenged with BSE inoculum. Individual animals were killed after 8, 16, 24, 32, 40, 44 months post inoculum. KT: non-inoculated control animals at the time of inoculation of the other animals.

Prof. Groschup also provided his immunohistochemical analyses of the brain samples, in correlation with the clinical symptoms of the animals (see tab. 2).

Table 2: Pathogenesis study, immunohistochemistry and clinical stages
(data from Dr. Groschup, FLI, Isle of Riems)

Months *post infectum*	Animal no.	IHC	Clinical stage	our analysis
16 mpi	IT 07	-	0	
16 mpi	IT 28	-	0	+/-
24 mpi	IT 24	-	0	-
24 mpi	IT 26	+	0	-
32 mpi	IT 61	+	0-1	-
32 mpi	IT 43	+++	2	++
40 mpi	IT 13	+++	2-3	++
44 mpi	IT 15	+++	3	++

IHC: immunohistochemistry
Clinical stages: 0 - no abnormality detected, 1 - possibly BSE, 2 - probably BSE, 3 - definitely BSE

De novo and seeded fibrilisation of rec PrP:

Seeded aggregation is a topic in this research program to amplify the signal from PrP^{Sc}-particles in surface-FIDA. It was proposed to test if the PrP^{Sc}-particles, which are detected in normal surface-FIDA directly by labelled antibodies, can be used as specific seeds for fibril formation of recPrP in the solution. A higher signal should be expected. First, seeding and fibrillogenesis had to be optimised before the fibrillogenesis from surface-bound seeds can be tested.

De novo fibrilisation of sheep recPrP and seeded fibrilisation with Scrapie prions from sheep

We study spontaneous and seeded fibrilisation. We varied the SDS-concentration to get optimal fibrillogenesis conditions for sheep recPrP(25-233). Fibrillogenesis of ovine recPrP(25-233) occurs only in presence of 250 mM NaCl and 0.02% SDS (10 mM NaPi, 150 ng/µl recPrP). (Fig. 31). At higher or lower SDS concentrations fibrillogenesis competes with other aggregation reactions like production of amorphous aggregates, which has been shown for hamster PrP within another project (Stohr et al. 2008). We verified the growth of amyloid fibrils via ThT assay, and electron microscopy (Fig. 32). We analysed SDS-concentrations from 0.01 to 0.06% SDS. Only at 0.02% SDS we could obtain amyloid fibrils after a minimum incubation period of 4 weeks (shaking at 650 rpm, 37°C).
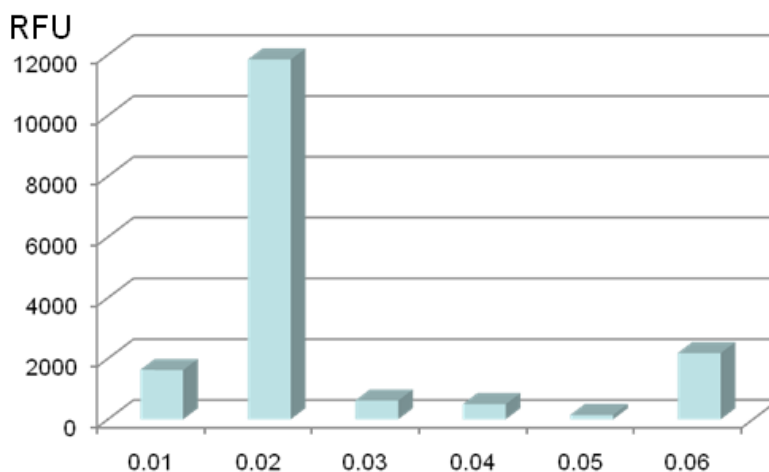
Fig. 31
Establishment of the optimal SDS concentration for sheep recPrP fibril formation ThT-assay of 150 ng/µl PrP sheep recPrP(25-233) in 10 mM NaPi 250 mM NaCl in different SDS concentrations.

Fig. 32
Electromicrograms of sheep rec PrP fibrils
(scale bar = 50 nm)

Furthermore we characterized the secondary structure of the pre-amyloid state (0.02% SDS) via circular dichroism spectroscopy (Fig 33). The secondary structure of the pre-amyloid state is dominated by alpha-helical and random coiled structures.
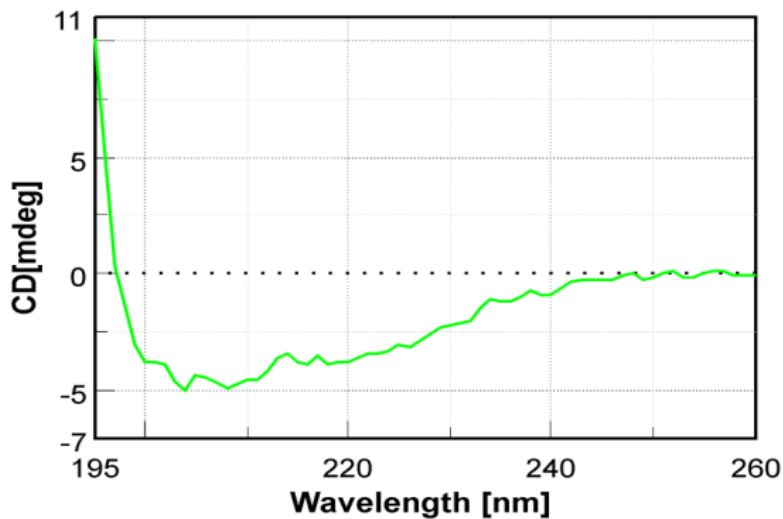
Fig. 33
Secondary structure of the pre amyloid state of sheep rec PrP.
Sheep rec PrP after incubation of a few hours in 0.02% SDS, 10 mM NaPi 250 mM NaCl. This samples formed fibrils after six weeks of incubation.

After adjusting the SDS concentration for the spontaneous fibrillogenesis, we assigned the results to the seeded aggregation. The preparation of sheep prion seeds via PTA was performed as shown above. We incubated the prion seed with recPrP as substrate in presence of 250 mM NaCl and 10 mM NaPi and monitored the forming of amyloid fibrils using ThT over a time period of 64h. Higher or lower SDS-concentrations did not lead to seeded aggregation of sheep recPrP(25-233).The optimal sheep recPrP concentration was lower than in the spontaneous system. Only 40 ng/µl sheep recPrP(25-233) was sufficient to distinguish positive and negative samples.

We could show a seed-induced, fast fibril formation using 40 ng/µl sheep recPrP(25-233) as substrate and prepurified sheep PrP^{Sc} as seed (fig. 34). Under this condition no increase of the fluorescence could be obtained for the control. We used the corresponding treated sample of brain homogenate of a healthy sheep as control in the recPrP sample.
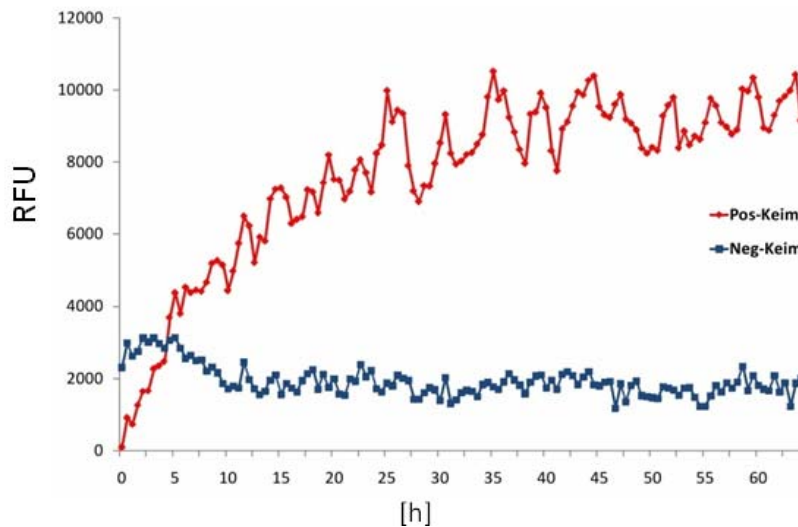
Fig. 34 seeded aggregation of sheep rec PrP Natural sheep PrP^{Sc} was used as seed and sheep rec PrP(25-233) was used as substrate.

The results show us that it will be possible to enlarge the size or the number of prion protein particles when our prion preparation procedures will be combined with the seeded amplification procedure. This combination can be tested in solution or on the chip surface.

Furthermore we established seeded aggregation of sheep recPrP using prepurified blood plasma of Scrapie infected sheep as seed. The plasma was prepurified as described above. The seeding conditions were those we used for seeded aggregation using prepurified brain tissue as seed. In fig. 35 the time course of ThT fluorescence is shown. Although the curve shows a lot of scatter, it is clearly shown that the sample from blood of infected sheep induces a seeded fibrillisation. Thus, seeding can be initiated by blood samples.
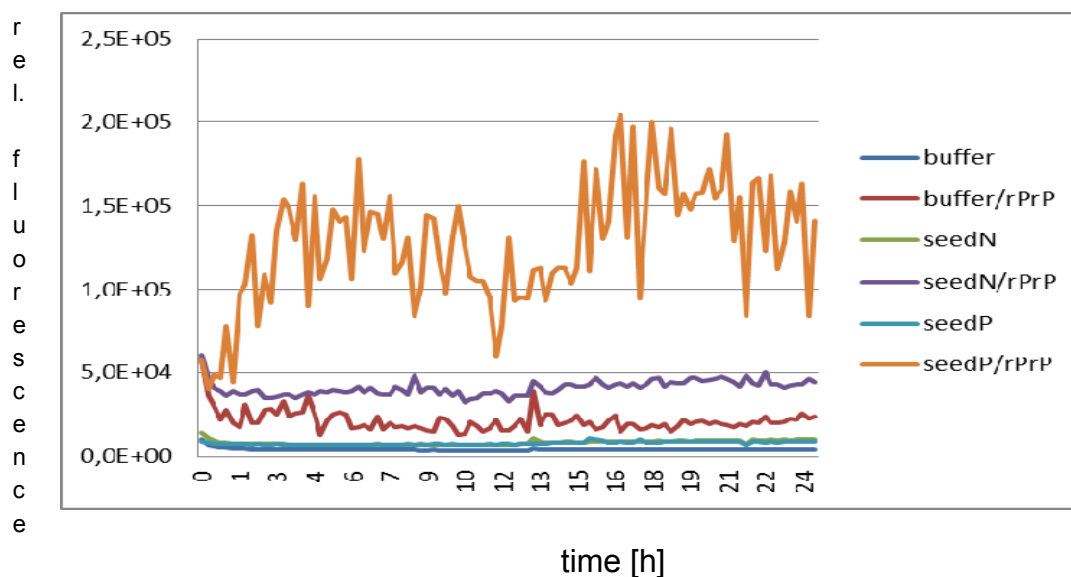
Fig. 35 seeded aggregation of Sheep recPrP using prepurified blood plasma of Scrapie infected sheep as seed
seed: prepurified plasma using PTA-precipitation, plasma from Scrapie infected sheep (seedP), plasma from healthy control (seedN). Recombinant sheep PrP (rPrP)

We applied these seeded samples to the surface-FIDA assay (fig. 36). To avoid background signals due to the soluble template recPrP, we carried out a 14.000 g centrifugation step and applied the pellet fraction to the surface-FIDA approach using ThT as detection dye for fibrils as described above. RecPrP background could not be avoided completely as could be seen in the comparison of the buffer control (PBS) with and without recPrP. Our interpretation is that recPrP formed disordered aggregates during the incubation time. This could also have happened in the negative control (Pnegativ/rPrP). But we can clearly see a much higher signal in the sample, which is seeded by blood plasma prions. Therefore we could deliver the proof of principle that the combination of surface-FIDA and PPA leads to significant signals, which still can be further improved in the future.
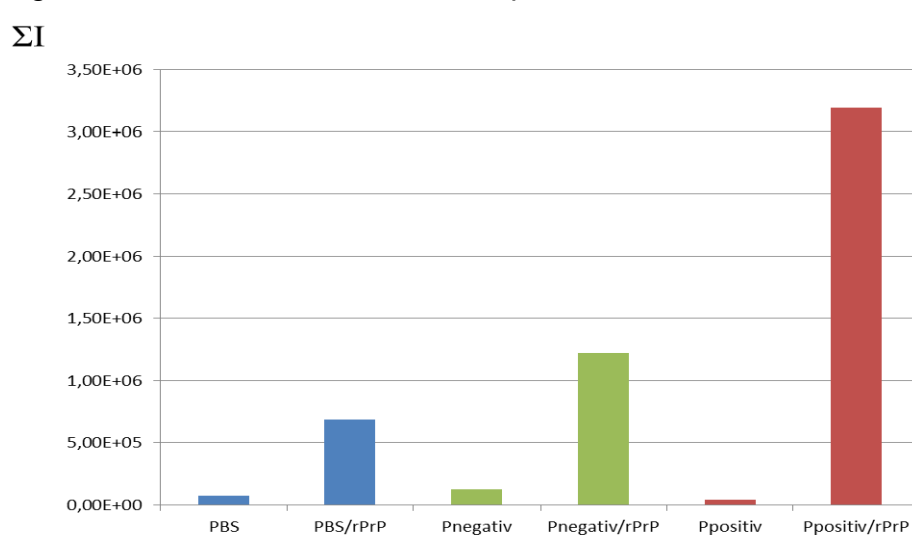
Fig. 36 Seeded aggregation combined with surface FIDA
Samples were applied to surface FIDA and analysed by ThT specific channel wavelength.
rPrP: recombinant sheep PrP, Pnegative: prepurified plasma using PTA-precipitation,
Ppositiv plasma from Scrapie infected sheep

De novo fibrilisation of cattle rec PrP and seeded fibrilisation with BSE-seeds

We analysed the secondary structure of bovine recPrP at different SDS concentrations by CD-spectroscopy (fig. 37A) at 0.1%, 0.04%, and 0.03% SDS under so called pre-amyloid conditions. Pre-amyloid conditions include partial denaturation of recPrP, which is a conformation preferable for fibrilisation. The secondary structure of bovine recPrP exhibits a mixture of random coil alpha-helix contents and very little beta-sheet content very similar to the earlier described pre-amyloid state of recPrP(90–231) from Syrian hamster (Fig. 37C) (Stohr et al. 2008). Further diluting of SDS, i.e. to 0.02% and 0.01%, leads to a shift towards a beta-sheet-rich secondary structure at the expense of the random coil portion (Fig. 37A).
The N-terminal truncated form of the bovine recPrP, i.e. PrP (102– 241) does not show the same secondary structure like the full length bovine recPrP at 0.02% SDS in presence of 250 mM NaCl, but has a higher random coil content, similar to full-length PrP at 0.03% SDS (Fig. 37B). Unfortunately, availability of the N-terminal

truncated form of bovine recPrP was very limited; therefore we had to restrict our studies on the comparison of the amyloid forming conditions adjusted for full-length bovine recPrP (0.02% SDS, 250 mM NaCl).

In contrast to the bovine system the conformation of the N-terminal truncated rec SHaPrP (90–231) (Stohr et al. 2008), and the full length rec SHaPrP (23–231) (Fig. 37 B and C) are very similar when determined under amyloid forming conditions (0.03% SDS, 250 mM NaCl). Both are a mixture of alpha-helical and denatured structures and have only little content of beta-sheet secondary structure.
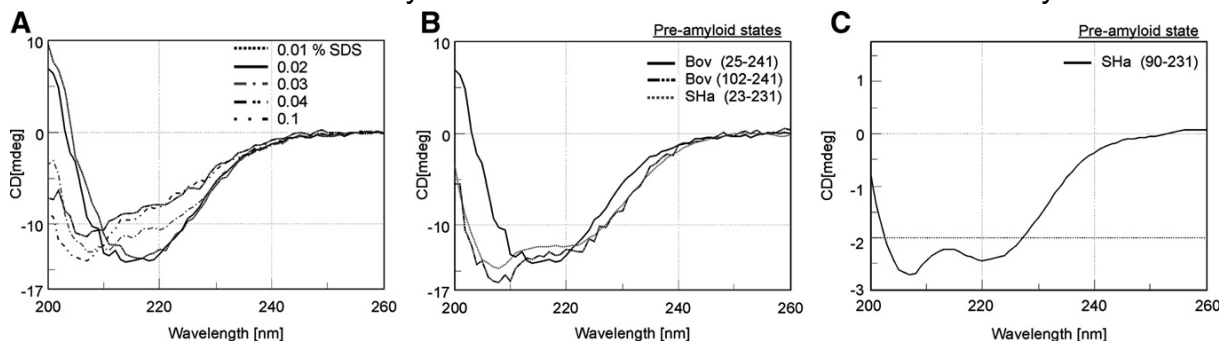
Fig. 37. Secondary structure analysis of the pre-amyloid state. CD-spectra were measured directly after adapting the SDS conditions, with a final concentration of 150 ng/µl PrP in 10 mMNaPi pH 7.4 and 250 mMNaCl. (A) CD-spectrum of bovine recPrP (25–241) in 0.01, 0.02, 0.03, 0.04, and in 0.1% SDS. (B) Pre-amyloid state of bovine recPrP (25–241) and bovine recPrP (102–241) (amyloid character after incubation proofed by ThT-assay; data not shown) were measured as described above in 0.02% SDS. Rec SHaPrP (23–231) (amyloid character after incubation proved by ThT-assay; data not shown) were measured as described above in 0.03% SDS. (C) Pre-amyloid state of rec SHaPrP (90–231) taken from Stohr et al. (2008), were measured as described above in 0.02% SDS and with a final concentration of 100 ng/µl PrP.

We varied the SDS-concentration to determine the optimal conditions for fibrillogenesis of bovine rec PrP(25-233). Fibrillogenesis of bovine rec PrP(25-241) occurs only in presence of 250 mM NaCl and 0.02% SDS (10 mM NaPi 150 ng/µl PrP). We verified the growth of amyloid fibrils via ThT assay (Fig. 38), congo red staining (Fig 39) and electron microscopy (EM) (Fig. 40). We analysed via ThT assay and EM the SDS-concentrations from 0.01 to 0.05% SDS. Only at 0.02% SDS we could obtain amyloid fibrils after a minimum incubation period of 1 week (shaking at 650 rpm, 37°C).
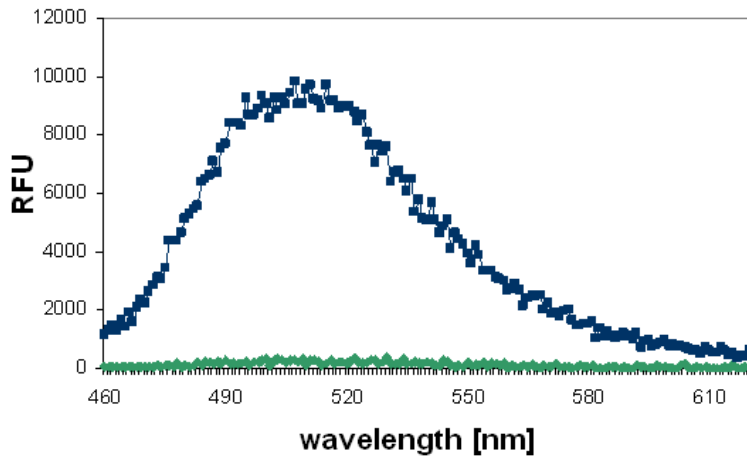
Fig 38 Bovine recPrP(25-241) fibrils
ThT was added to a final concentration of 5 µM and a final protein concentration of 150 ng/µl. The amyloid sample (blue line) shows the typical change in the emission spectrum compared to the buffer/ThT control (green line).
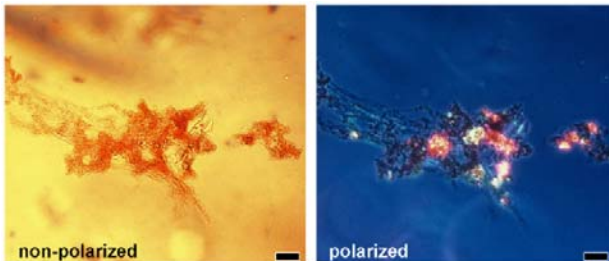
Fig 39
Bovine recPrP fibrils formed in 0.02% SDS were stained with Congo red and analysed by light microscopy using polarized and non-polarized light (bar = 20 µm).
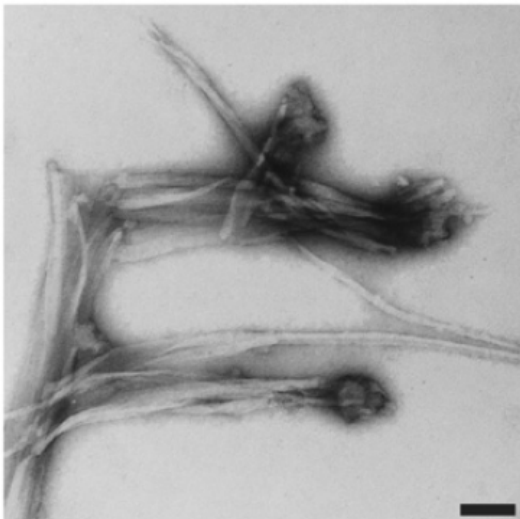
Fig 40
Electron micrograph showing the typical structure of amyloid fibrils after 7 days of incubation in 0.02% SDS (bar = 100 nm).

The conclusions from these results are similar to those achieved with the experiments in the ovine system. We expect, however, that amplification might be needed for the bovine system, whereas prions in sheep plasma are detectable without amplification in the surface-FIDA assay.

After adjusting the SDS-concentrations for the spontaneous fibrillogenesis, we assigned the results to the seeded aggregation. We monitored the amyloid fibril formation using ThT fluorescence when the seed was incubated in presence of 250 mM NaCl, 10 mM NaPi and 80 ng/µl bovine recPrP(25-241) as substrate over a time period of 65h. A concentration of 0.02% SDS was found optimal, higher or lower SDS-concentrations did not lead to seeded aggregation of bovine recPrP(25-241) (figure 42). A seed-induced, fast fibril formation with prepurified sheep PrP^{Sc} as seed is shown in figure 41. Only little increase in the fluorescence was observed in Scrapie-negative controls (figure 41).
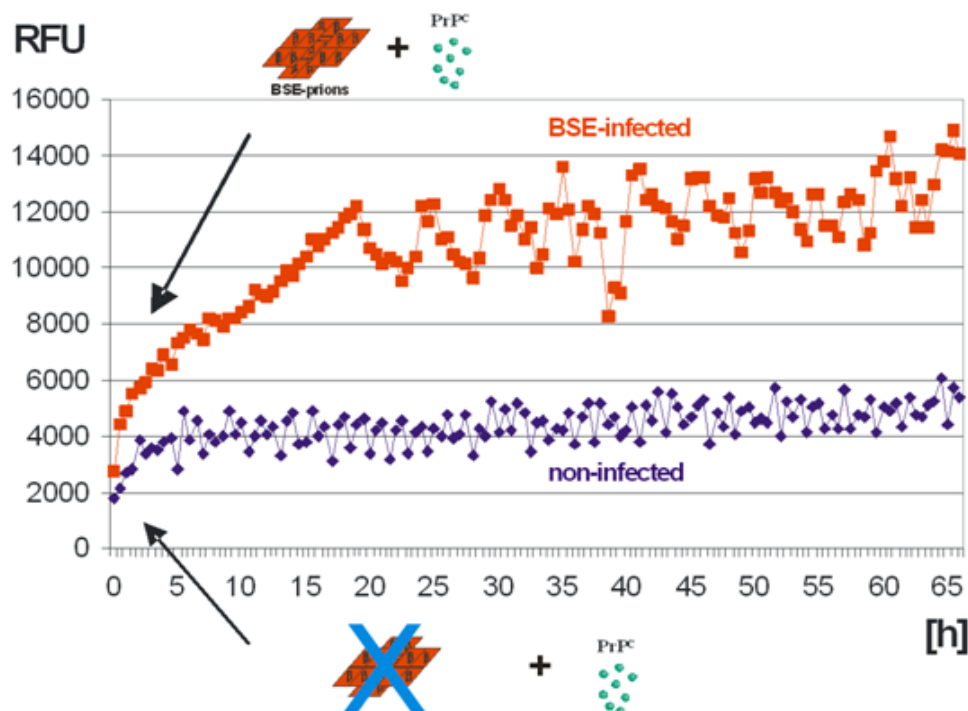
Figure 41: Seeded fibril formation. Fibril formation of bovine recPrP(25-241) was seeded with BSE-prions from brain tissue (red) or identically treated non-infected brain tissue (blue). The panel shows the time-dependent increase of fluorescence intensity. Samples containing BSE-prions can clearly be distinguished from non-infected controls.
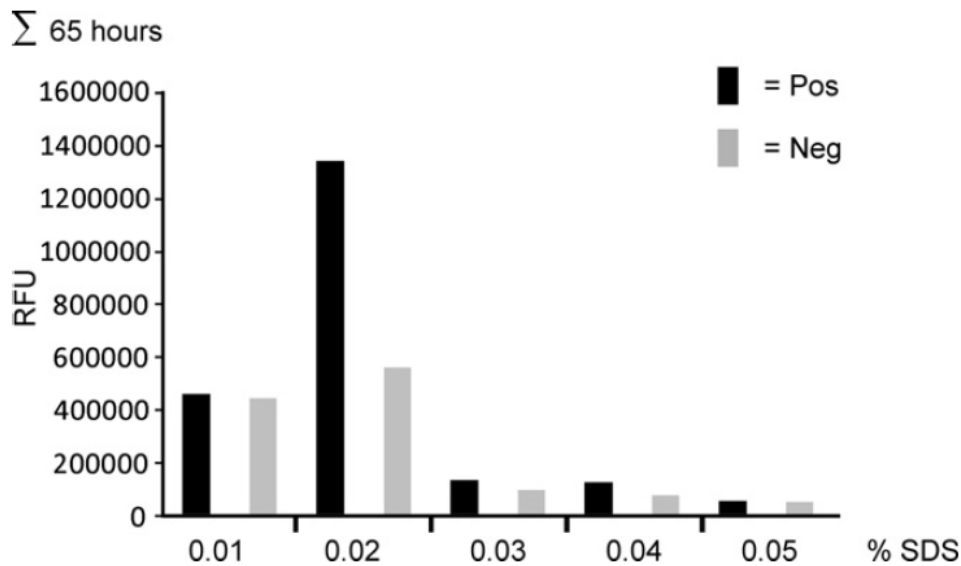
Fig. 42 Dependence of the amyloid seeding on SDS concentration. Amyloid formation in the seeding assay was monitored using ThT. The fluorescence signals were recorded every 30 min at 37° C and added after 65 h. SDS was varied from 0.01% to 0.05% SDS under otherwise constant buffer conditions (10 mM NaPi, pH 7.4, 250 mM NaCl, 80 ng/µl bovine recPrP(25-241)).Pos: seeds from infected samples, Neg: seeds from non-infected samples

Combination of seeded aggregation and surface-FIDA

We successfully combined surface-FIDA using one fluorescent labelled antibody as probe for PrP and ThT as probe for fibrils. ThT changes its emission spectrum specifically after binding the fibrils. It is used in the seeding experiments to identify fibril formation. We analysed amorphous aggregates of sheep rec PrP (without NaCl in the buffer during aggregation as described by Leffers et al. (2005) and fibrils . Our device allows for two channel detection (at 488 nm and 633 nm) (fig. 43). Thus we used Alexa-633-labelled antibody L42 and ThT as probes for fibril detection. A set of filters was installed to extract a 458 nm laserline, which is near to the excitation maximum of ThT in the fibril-bound state. Feasibility of ThT imaging was evaluated with recombinant ovine PrP fibrils. Amorphous prion protein aggregates were employed as negative controls in order to estimate the specificity of ThT-Binding. As shown in the figure below, both fibrils and amorphous aggregates, respectively, yield a signal in the antibody channel (A and D). However, only fibrils exhibit ThT-specific signals (B), which colocalize with the antibody signals (C). In contrast, disordered aggregates hardly bind any ThT (E, F).
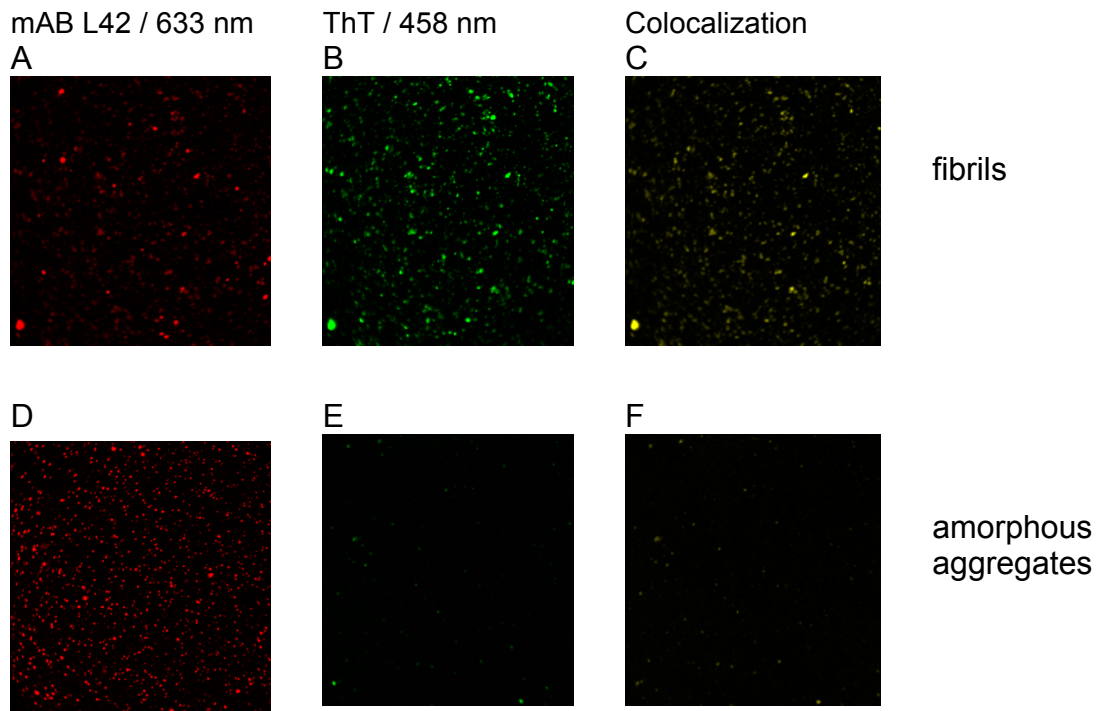
Fig. 43 Surface-FIDA of fibril and amorphous aggregates of sheep recPrP
antibody channel (A and D), ThT channel (B and E), Colocalization of both channels
(C and F)

Discussion

PrP^{Sc} as disease marker

Today prions are generally accepted as the agent of TSE infections; only a small number of scientists are still questioning this. Prions consist of PrP^{Sc} which is the pathogenic isoform of the host encoded prion protein PrP. It is well known that the applicant has defended the prion model for many years; it should be noted, however, that in the present work PrP^{Sc} is used as the unequivocal marker for TSE disease, independent upon the nature of the infectious agent. To our knowledge all scientists agree that a TSE-infection is strictly correlated with the presence of PrP^{Sc}. Some cases, where PrP^{Sc} could not be detected in an infected animal, could be explained by the fact, that the bioassay was more sensitive than the test for PrP^{Sc} at that time . PrP^{Sc} is composed of proteinase (PK)-resistant PrP^{Sc} (resPrP^{Sc}) and of protease-sensitive PrP^{Sc} (senPrP^{Sc}). The non-pathogenic, *i.e.* the cellular isoform, PrP^C, is entirely sensitive to PK-digestion. Today, most diagnostic approaches for TSE are based on the detection of the resPrP^{Sc} portion only; the concentration of PrP is determined by an antibody test (Western blot or ELISA), after all sensitive PrP was digested by PK. Several approaches have been followed to overcome the limitations of "PK-resistance" tests, which have been applied so far as *post mortem* tests and samples from brain tissue were used. Surrogate markers monitor a cellular reaction following the primary infection; they may be appropriate for special applications but are not very promising for diagnosis in the preclinical state. PrP^{Sc} conformation is characterized by secondary, tertiary and quaternary structure. Several tests described in the literature are based on testing PrP^{Sc}-specific secondary and/or tertiary structure like PrP^{Sc}-specific antibodies (Paramithiotis et al. 2003), PrP^{Sc}-conformation dependent immunoassays (Safar et al. 1998; Safar et al. 2002) or other PrP^{Sc}-binders like peptide ligands or heterocyclic compounds. The present work was directed to test the PrP^{Sc}-specific quaternary structure, *i.e.* the state of aggregation. Whereas PrP^C is soluble in the presence of mild detergents and does not bind more than one or two antibody molecules, the disease associated PrP^{Sc} is always insoluble in mild detergents, forms large aggregates and can bind many antibody molecules. As mentioned above, PrP^{Sc} embodies a PK-resistant and PK-sensitive portion which can differ dramatically not only between species, but also between individual animals and even within tissues of one animal. Thus we chose to detect total PrP^{Sc}, which correlates unequivocally with the disease.

Optimization of surface-FIDA in respect to sensitivity and specificity of detecting single PrP^{Sc}-particles

The method was adapted to cattle BSE and sheep Scrapie. First steps of optimization were directed to the preparation of PrP^{Sc} particles. Optimal conditions for PTA precipitation of PrP^{Sc} particles leaving PrP^C soluble were established for each

species: sheep and cattle and for the origin of the material: brain tissue, CSF, blood plasma, and PBMC. The surface capture procedure was optimised by covalent linkage of the capture antibody to the glass surface instead of the adhesive binding used before and allowed us more stringent washing steps. We optimised the blocking and washing steps for different sample materials and species, respectively. These washing steps were essential to remove residual impurities bound to the capture surface(?). We improved the washing steps after sample and antibody incubation, respectively. These optimizations were performed using PrP particles enriched by PTA precipitation from brain tissue as well as from body fluids of sheep and cattle.

Enrichment of PrP^{Sc} particles in blood and other body fluids

We applied precipitation and centrifugation steps to enrich PrP^{Sc} particles in a volume applicable to surface-FIDA. Therefore we adapted PTA precipitation to brain tissue, CSF and blood fractions which contain PrP^{Sc} particles. Blood was fractionated in plasma and PBMC and these different fractions were tested by surface-FIDA. The methods to prepare PrP^{Sc}-particles from different body fluids and from different species (sheep, cattle) were tested and only small changes in the sarkosyl concentration were necessary. We want to point out, that the use of lipase in the pre-purification procedure of plasma samples turned out to be important for efficient detection of PrP-aggregates in blood plasma. The distribution of PrP aggregates is different in blood samples of cattle and sheep. We were able to detect PrP aggregates in plasma of Scrapie-infected sheep, but not in BSE-infected cattle. This corresponds to the findings of other groups that PrP^{Sc} in sheep is distributed to more organs as compared to cattle. Moreover, blood from Scrapie sheep is infectious (Houston et al. 2008), whereas blood from BSE cattle is not (World Health Organization, 2006). A particular advantage of surface-FIDA is, that other methods for preparation of PrP^{Sc}-particles can be combined with the detection steps.

Application of surface-FIDA to body fluids like CSF and blood fractions

We used body fluids like CSF, blood plasma and PBMC, because these body fluids can be taken from living animals. In the first step we tested body fluids from animals in the clinical state of disease to evaluate which body fluids principally are adaptable to surface FIDA and to establish a preparation of the different body fluids. The data we obtained for CSF of cattle are very promising, but have to be improved with a larger sample set and confirmed in a test series. On the other side we have to take into account that the applicability of CSF as a BSE diagnostic is low. Our main effort was to detect PrP^{Sc} particles in blood samples from Scrapie-infected sheep and BSE-infected cattle, because blood is more applicable to diagnostic tests of animals. The first step was to test blood fractions from sheep since according to the literature the concentration of PrP^{Sc} in blood from sheep is higher as compared to cattle. Blood was fractionated in blood plasma and PBMC. We tested both fractions from sheep in

the clinical state and were able to detect prion particles by surface-FIDA. We were not able to detect prion particles in plasma of BSE-infected cattle.

Evaluation of the sensitivity limit of surface-FIDA in respect to the preclinical state of disease

We examined brain samples from BSE cattle with the objective to apply surface-FIDA to diagnose preclinical animals. We obtained samples of brain tissue and blood plasma from the pathogenesis study at the Friedrich-Loeffler-Institute. The preparation of the samples was done as for material of animals in the clinical state of the disease.

As expected we were not able to detect any prion particles in the blood samples. But we were able to detect preclinical cattle using brain tissue. We conclude from our results in combination with the results from bioassays that blood is not a promising source for future test developments. As described above, we could detect prion particles in plasma of Scrapie infected sheep. We got a blinded sample set of sheep plasma samples from the VLA archive containing samples from clinical, preclinical and healthy sheep. We analysed these samples and estimated sample identity as described in the result chapter. Although the intensity evaluation resulted in identification of some pre-clinical cases with only one false positive, we failed to identify the clinical animals. This might be due to instrumental or sample issues, as pointed out above.

Enhancement of PrP^{Sc}-particles by prion protein amplification

We found that prion protein amplification (PPA) carried out with PrP^{Sc}-particles from Scrapie-sheep as seeds and recPrP as substrate improved our detection system. In an earlier study, we established PPA with highly purified compounds, SHa recPrP as monomers and PTA precipitated PrP^{Sc} from SHa scrapie brain tissue (Stohr et al. 2008). These studies were directed to elucidate the mechanism of amplification. We adapted this type of PPA to natural Scrapie in sheep and BSE in cattle. In the first step the conditions for *de novo* fibrillogenesis of bovine (Panza et al. 2008) and sheep recPrP (Panza et al. 2010) were evaluated. After that, seeded aggregation was established with purified PrP^{Sc} particles from brain tissue of Scrapie-infected sheep and BSE-infected cattle. Finally we were able to use prepurified sheep plasma samples for seeding. We combined surface FIDA and PPA by using the fibril specific dye ThT. Therefore we established surface-FIDA by using ThT instead of a fluorescent antibody to be able to differentiate between fibrils and unspecific amorphous aggregates. We were able to detect seed-induced fibrils of ovine PrP after seeding with pre-purified Scrapie sheep plasma.

We had two options for combining seeded aggregation and surface-FIDA. Either the amplification is carried out in solution, or the seeds when bound to the surface will be

enlarged drastically. We decided to achieve the signal enhancement by seeded aggregation in solution, and after that applying surface-FIDA.

In the future we will adopt our surface-FIDA assay to other prion diseases especially Creutzfeldt-Jakob disease and chronic wasting disease. Concerning Creutzfeldt Jakob disease we expect major impact of our findings in the preparation of blood samples as well as the development steps in the surface-FIDA approach.

Furthermore we started to adopt our assay to the detection of protein aggregates occurring in other neurodegenerative diseases e.g. Alzheimers diseases (abeta-aggregates) and Parkinson's disease (alpha-synuclein aggregates).

And finally we will develop our assay in the direction of high optical resolution using new physical techniques like STORM, PAINT, STED, to analyse if we could differentiate different types of aggregates or oligomers and correlate them to diseases progression or enhance the sensitivity of our assay.

References

Atarashi R, Satoh K, Sano K, Fuse T, Yamaguchi N, Ishibashi D, Matsubara T, Nakagaki T, Yamanaka H, Shirabe S et al. 2011. Ultrasensitive human prion detection in cerebrospinal fluid by real-time quaking-induced conversion. *Nat Med* **17**(2): 175-178.

Birkmann E, Henke F, Weinmann N, Dumpitak C, Groschup M, Funke A, Willbold D, Riesner D. 2007. Counting of single prion particles bound to a capture-antibody surface (surface-FIDA). *Vet Microbiol* **123**(4): 294-304.

Birkmann E, Schafer O, Weinmann N, Dumpitak C, Beekes M, Jackman R, Thorne L, Riesner D. 2006. Detection of prion particles in samples of BSE and scrapie by fluorescence correlation spectroscopy without proteinase K digestion. *Biol Chem* **387**(1): 95-102.

Buschmann A, Groschup MH. 2005. Highly bovine spongiform encephalopathy-sensitive transgenic mice confirm the essential restriction of infectivity to the nervous system in clinically diseased cattle. *J Infect Dis* **192**(5): 934-942.

Edgeworth JA, Farmer M, Sicilia A, Tavares P, Beck J, Campbell T, Lowe J, Mead S, Rudge P, Collinge J et al. 2011. Detection of prion infection in variant Creutzfeldt-Jakob disease: a blood-based assay. *Lancet* **377**(9764): 487-493.

Foster JD, Wilson M, Hunter N. 1996. Immunolocalisation of the prion protein (PrP) in the brains of sheep with scrapie. *Vet Rec* **139**(21): 512-515.

Grosset A, Moskowitz K, Nelsen C, Pan T, Davidson E, Orser CS. 2005. Rapid presymptomatic detection of PrPSc via conformationally responsive palindromic PrP peptides. *Peptides* **26**(11): 2193-2200.

Houston F, McCutcheon S, Goldmann W, Chong A, Foster J, Siso S, Gonzalez L, Jeffrey M, Hunter N. 2008. Prion diseases are efficiently transmitted by blood transfusion in sheep. *Blood* **112**(12): 4739-4745.

Laemmli UK, Beguin F, Gujer-Kellenberger G. 1970. A factor preventing the major head protein of bacteriophage T4 from random aggregation. *J Mol Biol* **47**(1): 69-85.

Leffers KW, Wille H, Stohr J, Junger E, Prusiner SB, Riesner D. 2005. Assembly of natural and recombinant prion protein into fibrils. *Biol Chem* **386**(6): 569-580.

Muller H, Stitz L, Wille H, Prusiner SB, Riesner D. 2007. Influence of water, fat, and glycerol on the mechanism of thermal prion inactivation. *J Biol Chem* **282**(49): 35855-35867.

Murayama Y, Yoshioka M, Okada H, Takata M, Yokoyama T, Mohri S. 2007. Urinary excretion and blood level of prions in scrapie-infected hamsters. *J Gen Virol* **88**(Pt 10): 2890-2898.

Panza G, Luers L, Stohr J, Nagel-Steger L, Weiss J, Riesner D, Willbold D, Birkmann E. 2010. Molecular interactions between prions as seeds and recombinant prion proteins as substrates resemble the biological interspecies barrier in vitro. *PLoS One* **5**(12): e14283.

Panza G, Stohr J, Dumpitak C, Papathanassiou D, Weiss J, Riesner D, Willbold D, Birkmann E. 2008. Spontaneous and BSE-prion-seeded amyloid formation of full length recombinant bovine prion protein. *Biochem Biophys Res Commun* **373**(4): 493-497.

Paramithiotis E, Pinard M, Lawton T, LaBoissiere S, Leathers VL, Zou WQ, Estey LA, Lamontagne J, Lehto MT, Kondejewski LH et al. 2003. A prion protein epitope selective for the pathologically misfolded conformation. *Nat Med* **9**(7): 893-899.

Pitschke M, Prior R, Haupt M, Riesner D. 1998. Detection of single amyloid beta-protein aggregates in the cerebrospinal fluid of Alzheimer's patients by fluorescence correlation spectroscopy. *Nat Med* **4**(7): 832-834.

Rubenstein R, Chang B, Gray P, Piltch M, Bulgin MS, Sorensen-Melson S, Miller MW. 2010. A novel method for preclinical detection of PrPSc in blood. *J Gen Virol* **91**(Pt 7): 1883-1892.

Saborio GP, Permanne B, Soto C. 2001. Sensitive detection of pathological prion protein by cyclic amplification of protein misfolding. *Nature* **411**(6839): 810-813.

Safar J, Wille H, Itri V, Groth D, Serban H, Torchia M, Cohen FE, Prusiner SB. 1998. Eight prion strains have PrP(Sc) molecules with different conformations. *Nat Med* **4**(10): 1157-1165.

Safar JG, Scott M, Monaghan J, Deering C, Didorenko S, Vergara J, Ball H, Legname G, Leclerc E, Solforosi L et al. 2002. Measuring prions causing bovine spongiform encephalopathy or chronic wasting disease by immunoassays and transgenic mice. *Nat Biotechnol* **20**(11): 1147-1150.

Safar JG, Wille H, Geschwind MD, Deering C, Latawiec D, Serban A, King DJ, Legname G, Weisgraber KH, Mahley RW et al. 2006. Human prions and plasma lipoproteins. *Proc Natl Acad Sci U S A* **103**(30): 11312-11317.

Soto C, Saborio GP, Anderes L. 2002. Cyclic amplification of protein misfolding: application to prion-related disorders and beyond. *Trends Neurosci* **25**(8): 390-394.

Sternberg SR. 1983. BIOMEDICAL IMAGE PROCESSING. *Computer* **16**(1): 22-34.

Stohr J, Weinmann N, Wille H, Kaimann T, Nagel-Steger L, Birkmann E, Panza G, Prusiner SB, Eigen M, Riesner D. 2008. Mechanisms of prion protein assembly into amyloid. *Proc Natl Acad Sci U S A* **105**(7): 2409-2414.

Terry LA, Howells L, Hawthorn J, Edwards JC, Moore SJ, Bellworthy SJ, Simmons H, Lizano S, Estey L, Leathers V et al. 2009. Detection of PrPsc in blood from sheep infected with the scrapie and bovine spongiform encephalopathy agents. *J Virol* **83**(23): 12552-12558.

Thackray AM, Fitzmaurice TJ, Hopkins L, Bujdoso R. 2006. Ovine plasma prion protein levels show genotypic variation detected by C-terminal epitopes not exposed in cell-surface PrPC. *Biochem J* **400**(2): 349-358.

Thorne L, Terry LA. 2008. In vitro amplification of PrPSc derived from the brain and blood of sheep infected with scrapie. *J Gen Virol* **89**(Pt 12): 3177-3184.

Wille H, Shanmugam M, Murugesu M, Ollesch J, Stubbs G, Long JR, Safar JG, Prusiner SB. 2009. Surface charge of polyoxometalates modulates polymerization of the scrapie prion protein. *Proc Natl Acad Sci U S A* **106**(10): 3740-3745.

World Health Organization. 2006. WHO Tables on Tissue Infectivity Distribution in Transmissible Spongiform Encephalopathies. http://www.who.int/bloodproducts/tablestissueinfectivity.pdf

Signature   _____   Name (block capitals)   _____

Date   _____   Position   _____